PPARβ/δ attenuates palmitate-induced endoplasmic reticulum stress and induces autophagic markers in human cardiac cells

Xavier Palomer[a], Eva Capdevila-Busquets[a], Gaia Botteri[a], Laia Salvadó[a], Emma Barroso[a], Mercy M. Davidson[b], Liliane Michalik[c], Walter Wahli[c,d], Manuel Vázquez-Carrera[a,*]

[a]Department of Pharmacology and Therapeutic Chemistry, IBUB (Institut de Biomedicina de la Universitat de Barcelona) and CIBER de Diabetes y Enfermedades Metabólicas Asociadas (CIBERDEM), Faculty of Pharmacy, University of Barcelona, Diagonal 643, Barcelona E-08028, Spain

[b]Department of Radiation Oncology, Columbia University, P&S 11-451, 630 West 168th Street, New York, NY 10032, USA

[c]Center for Integrative Genomics, National Research Center Frontiers in Genetics, University of Lausanne, Quartier UNIL-Sorge, Bâtiment Génopode, CH-1015 Lausanne, Switzerland

[d]Lee Kong Chian School of Medicine, Nanyang Technological University, School of Nursing Building, SGH, Block C, #01-01, 9 Hospital Drive, Singapore 169612

***Corresponding author:** Department of Pharmacology and Therapeutic Chemistry, Faculty of Pharmacy, University of Barcelona, Diagonal 643, E-08028, Barcelona, Spain

E-mail: mvazquezcarrera@ub.edu, Phone: +34 934024531; Fax: +34 934035982

Acknowledgements

This study was supported by funds from the *Ministerio de Economía y Competitividad* of the Spanish Government (SAF2009-06939 and SAF2012-30708). *CIBER de Diabetes y Enfermedades Metabólicas Asociadas* (CIBERDEM) is an initiative of the *Instituto de Salud Carlos III* (ISCIII) - *Ministerio de Economía y Competitividad*. We thank the University of Barcelona's Language Advisory Service for their assistance.

The authors of this manuscript have certified that they comply with the Principles of Ethical Publishing in the International Journal of Cardiology.

Disclosure statement

None of the authors has any conflict of interest to disclose.

Keywords: Autophagy; Diabetic cardiomyopathy; Endoplasmic reticulum stress; PPARβ/δ

ABSTRACT

Background: Chronic endoplasmic reticulum (ER) stress contributes to the apoptotic cell death in the myocardium, thereby playing a critical role in the development of cardiomyopathy. ER stress has been reported to be induced after high-fat diet feeding in mice and also after saturated fatty acid treatment in vitro. Therefore, since several studies have shown that peroxisome proliferator-activated receptor (PPAR)β/δ inhibits ER stress, the main goal of this study consisted in investigating whether activation of this nuclear receptor was able to prevent lipid-induced ER stress in cardiac cells.

Methods and results: Wild-type and transgenic mice with reduced PPARβ/δ expression were fed a standard diet or a high-fat diet for two months. For in vitro studies, a cardiomyocyte cell line of human origin, AC16, was treated with palmitate and the PPARβ/δ agonist GW501516. Our results demonstrate that palmitate induced ER stress in AC16 cells, a fact which was prevented after PPARβ/δ activation with GW501516. Interestingly, the effect of GW501516 on ER stress occurred in an AMPK-independent manner. The most striking result of this study is that GW501516 treatment also upregulated the protein levels of beclin 1 and LC3II, two well-known markers of autophagy. In accordance with this, feeding on a high-fat diet or suppression of PPARβ/δ in knockout mice induced ER stress in the heart. Moreover, PPARβ/δ knockout mice also displayed a reduction in autophagic markers.

Conclusion: Our data indicate that PPARβ/δ activation might be useful to prevent the harmful effects of ER stress induced by saturated fatty acids in the heart by inducing autophagy.

1. Introduction

If uncorrected, type 2 diabetes and obesity are among the major risk factors for the development of cardiovascular diseases. Plasma free fatty acid levels are often elevated in patients with type 2 diabetes mellitus or obesity, and are responsible for several harmful effects on the heart, such as the activation of endoplasmic reticulum (ER) stress and chronic low-level inflammatory processes. In fact, it has been suggested that saturated fatty acids induce insulin resistance by causing ER stress in pancreatic β-cells [1,2], hepatocytes [3] and muscle cells [4,5] of human and murine origin. ER is the organelle responsible for protein folding and maturation in eukaryotic cells. Any physiological or pathological perturbation that interferes with the folding process will cause the accumulation of unfolded or misfolded proteins, thus leading to the activation of the unfolded protein response (UPR) by the ER [6]. Initiation of the UPR involves three key signalling proteins: activating transcription factor 6 (ATF6), inositol-requiring enzyme (IRE)-1α, and PKR-like ER kinase (PERK). In the absence of stress, the N-termini of these trans-membrane proteins are bound to the intra-luminal BiP/GRP78 (binding immunoglobulin protein/glucose-regulated protein 78) protein. On stress exposure, the large excess of unfolded proteins sequesters BiP/GRP78 from trans-membrane ER proteins, thereby inducing the UPR. In particular, ATF6 is transported from the ER to the Golgi complex, where proteolytic cleavage releases a soluble fragment that translocates to the nucleus, in which it acts as a transcription factor for ER chaperones [7]. In addition, the endoribonuclease activity of IRE-1α cleaves a 26 base-pair segment from the mRNA of the X-box binding protein-1 (*XBP1*), creating an alternative message that is translated into the spliced and active form of this transcription factor, sXBP1. Finally, PERK phosphorylates and inhibits the eukaryotic initiation factor 2α (eIF2α), and by this means inhibits the translation of most mRNAs [8]. However, some mRNAs escape this translational control, for example transcription factor *ATF4*, a master regulator of the ER stress response that is capable of inducing the expression of *ATF3*, *BiP/GRP78*, *CHOP* (CCAAT/enhancer binding protein homologous protein) and genes involved in autophagy, antioxidant responses, and apoptosis [9].

Activation of the UPR initially aims to mitigate adverse effects of ER stress and thus enhance cell survival by halting general mRNA translation, facilitating protein degradation via the ER-associated

degradation (ERAD) pathway and enhancing the production of molecular chaperones involved in protein folding. If ER stress is limited, the UPR will potentiate autophagy to protect the cells [10]. This pro-survival pathway has evolved as an alternate mechanism for saving nutrients, recycling intracellular components and eliminating abnormal protein aggregates and misfolded proteins formed during the ER stress that cannot be removed through the ERAD pathway. However, if ER stress is not mitigated within a certain time period or the disturbance is prolonged, then, the UPR will turn on apoptosis for removing cells that threaten the integrity of the organism [11]. Cardiomyocytes rarely proliferate within the adult heart and, as a consequence, their loss due to apoptosis may play an essential pathogenic role during cardiovascular diseases [7]. In consonance with this, ER stress is involved in the pathogenesis of diabetic cardiomyopathy by enhancing cell death in the myocardium of streptozotocin-induced diabetic rats [12]. The myocardium of two rat models of type 2 diabetes mellitus also displays ER stress [13,14]. For this reason, inhibition of ER stress has been suggested as a potential therapeutic target for preventing and treating diabetic cardiomyopathy.

Peroxisome proliferator-activated receptor (PPAR)β/δ is a transcription factor that regulates cardiac metabolism and can limit myocardial inflammation and hypertrophy via inhibition of nuclear factor (NF)-κB [15]. NF-κB is a pro-inflammatory transcription factor that is activated in the heart during prolonged ER stress, and is responsible for the induction of apoptosis [16]. Cardiomyocyte-restricted deletion of PPARβ/δ decreases basal myocardial fatty acid oxidation, thus leading to lipotoxic cardiomyopathy and subsequent cardiac dysfunction, cardiac hypertrophy and congestive heart failure [17,18]. Interestingly, activation of PPARβ/δ with the GW501516 agonist rescues ER stress induced by palmitate in pancreatic β-cells [19], while another agonist, L165041, attenuates ER stress in liver [20], although the mechanisms involved remain unknown. Therefore, the present study was designed to gain a better understanding of the mechanisms by which exposure to the saturated fatty acid palmitate results in ER stress in cardiac cells. In addition, since PPARβ/δ is the most prevalent PPAR isoform in the heart [15], we also aimed to elucidate whether the PPARβ/δ agonist GW501516 could prevent saturated fatty acid-induced ER stress in cardiac myocytes, as well as the mechanisms involved.

2. Methods

2.1. Cell culture and mice

Human cardiac AC16 cells were maintained and grown as previously described [21]. Palmitate-containing medium was prepared by conjugation with fatty acid-free bovine serum albumin [22]. After incubation, RNA or protein was extracted from cardiac cells as described below.

Male PPARβ/δ-null mice and their control wild-type littermates with the same genetic background (C57BL/6X129/SV) were used (aged 3-5 months old) [23]. Each strain was randomized into two groups. One group was fed with a standard chow diet, and the other was fed with a Western-type high-fat diet (HFD, 45% Kcal from fat, 91.5% saturated fatty acid content) for 8 weeks. Mice were housed under standard light-dark cycle (12-h light/dark cycle) and temperature (21 ± 1ºC) conditions, and food and water were provided *ad libitum.* At the end of the treatment, mice were anaesthetized with 5% isoflurane and, after monitoring the adequacy of anaesthesia by testing rear foot reflexes, they were euthanized by cervical dislocation. After this, the heart was excised, rinsed in ice-cold phosphate buffer saline and snap-frozen in liquid nitrogen. All procedures were approved by the University of Barcelona Bioethics Committee, as stated in Law 5/21 July 1995 passed by the Generalitat de Catalunya.

2.2. RNA preparation and quantitative real-time RT-PCR analysis

Relative levels of specific mRNAs were assessed by real-time reverse transcription polymerase chain reaction (RT-PCR), as previously described [24]. The sequences of the forward and reverse primers are shown in Supplemental Table 1. For measurement of *XBP1* splicing, cDNA was used for PCR amplification using *XBP1* primers spanning the 26-bp intron splicing site (forward: ′5 -TGAGAACCAGGAGTTAAGAACACGC-3′ and reverse: 5′-TTCTGGGTAGACCTCTGGGAGTTCC-3′). The PCR cycle consisting of 94°C for 1 min, 62°C for 1 min, and 72°C for 1 min was repeated 30 times. This gave a PCR product of 326 bp for unspliced and 300 bp for spliced XBP1. The PCR products were separated by electrophoresis with a 2% agarose gel and visualized by ethidium bromide staining.

2.3. Immunoblot analysis

To obtain total protein extracts, AC16 cardiac cells and the heart tissue were lysed in cold RIPA buffer (Sigma, St Louis, MO, USA) with phosphatase and protease inhibitors (0.2 mmol/L

phenylmethylsulfonyl fluoride, 1 mmol/L sodium orthovanadate, 5.4 μg/mL aprotinin). The homogenate was then centrifuged at 10,000 x*g* for 30 min at 4°C, and protein concentration contained in the supernatant was determined using the Bradford method [25]. Protein extracts were separated by SDS-PAGE on 10% separation gels and transferred to Immobilon polyvinylidene difluoride membranes (Millipore, Bedford, MA, USA) [26]. Proteins were detected using the Western Lightning® Plus-ECL chemiluminescence kit (PerkinElmer, Waltham, MA, USA) and their size was estimated using protein molecular mass standards (Life Technologies, S.A., Spain). All antibodies used throughout the study were purchased from Cell Signaling Technology (Danvers, MA, USA), except actin (Sigma).

2.4. Statistical Analysis

Results are expressed as the mean ±SD of three independent experiments for the in vitro studies, each consisting of three culture plates (n=9), and of four mice for the in vivo experiments. Significant differences were established by one-way ANOVA using the GraphPad Prism (GraphPad Software Inc. V4.03, San Diego, CA, USA) software. When significant variations were found by one-way ANOVA, the Tukey-Kramer multiple comparison post-test was performed. Differences were considered significant at $P < 0.05$.

3. Results

3.1. PPARβ/δ activation prevents palmitate-induced ER stress in cardiac cells of human origin

As a first approach, we aimed to determine whether palmitate (0.25 mM for 18 h) was capable of inducing the expression of several ER stress markers in human cardiac AC16 cells. Real-time RT-PCR analyses demonstrated that palmitate significantly induced the expression of *sXBP1, ATF3* (approximately 2-fold, $P < 0.001$), *BiP/GRP78* (4.5-fold, $P < 0.001$) and *CHOP* (4.5-fold, $P < 0.001$), compared to cells exposed only to BSA (Fig. 1). To investigate whether PPARβ/δ activation prevented ER stress, human cardiac cells were co-incubated with palmitate and GW501516 (10 μM). As shown in Fig. 2A, the PPARβ/δ agonist completely abolished the increase in *ATF3* and attenuated the rise in *CHOP* expression caused by the saturated fatty acid, but did not prevent the splicing of *XBP1* or the induction of *BiP/GRP78* expression. In agreement with the above results, BiP/GRP78 and CHOP protein levels were increased in cells exposed to palmitate (Fig. 2B). Since activation of IRE-1α promotes the

splicing of *XBP1*, we also evaluated whether palmitate upregulated IRE-1α phosphorylation at Ser724 residues, which is indicative of its activity. As expected, palmitate treatment also enhanced the phosphorylation of IRE-1α with regard to control non-treated cells (2-fold, $P < 0.05$, Fig. 2B). On the contrary, no changes were observed in the phosphorylation levels at the Ser51 residue of eIF2α (see Supplemental Fig. 1A). Consistent with changes in mRNA levels, GW501516 abrogated the increase in CHOP protein levels induced by palmitate, but not those of the BiP/GRP78 chaperone. Surprisingly, GW501516 prevented IRE-1α phosphorylation induced by palmitate as well, although *sXBP1* was not downregulated. Incubation with GW501516 alone had no effect on *sXBP1* levels, but prevented IRE-1α phosphorylation in palmitate-treated cells. On the other hand, co-incubation of cells with palmitate, GW501516 and the PPARβ/δ antagonist GSK0660 (10 μM) reversed the effects of GW501516 on the expression of *ATF3*, but not on *CHOP* (Fig. 2A), therefore demonstrating that PPARβ/δ activation was involved, at least in part, in the effects of GW501516 on ER stress.

3.2. The preventive effect of PPARβ/δ activation on palmitate-induced ER stress is AMPK-independent

To investigate the role of 5' AMP-activated protein kinase (AMPK) in palmitate-induced ER stress in human cardiac cells, as well as the preventive effects of GW501516, we took advantage of the AMPK activator AICAR (5-aminoimidazole-4-carboxamide ribonucleotide) and the AMPK inhibitor compound C. As shown in Fig. 3A, the increase in the expression of the ER markers *sXBP1*, *BiP/GRP78* and *CHOP* caused by palmitate was abolished in cells co-incubated with palmitate plus AICAR. In contrast, AICAR further induced *ATF3* mRNA transcript levels (3.5-fold, $P < 0.001$ vs. control cells). In accordance with these data, AICAR prevented IRE-1α phosphorylation and the induction of BiP/GRP78 and CHOP protein levels stimulated by the saturated fatty acid (Fig. 3B), but appeared to up-regulate eIF2α phosphorylation on Ser51 residues (3-fold, $P < 0.01$ vs. control cells, Supplemental Fig. 1B). The outcome observed after co-incubation with compound C demonstrated the involvement of AMPK in ER stress induced by palmitate, since compound C abolished the effects of AMPK activation on *XBP1* splicing, ATF3 and CHOP mRNA expression and protein accumulation, and the phosphorylation of eIF2α and IRE-1α (Fig. 3 and Supplemental Fig. 1B). To further confirm the role of AMPK in regulating ER stress in our cells, we monitored AMPK phosphorylation at Thr172, which is essential for its activity.

As expected, compound C reduced AMPK phosphorylation (~90% reduction, $P < 0.05$ vs. control cells) in human AC16 cardiac cells but, strikingly, both AICAR (2-fold, $P < 0.05$ vs. control cells) and palmitate (3.5-fold, $P < 0.001$) enhanced this phosphorylation (Supplemental Fig. 2A). We also explored the phosphorylation of the cardiac-specific acetyl-CoA carboxylase (ACC) isoform, ACC2, a substrate for AMPK that serves as a surrogate for determining its activity. In contrast to AMPK phosphorylation, phospho-ACC2 levels were slightly reduced in cells exposed to palmitate or compound C, whereas in the presence of AICAR, they were significantly raised (2-fold, $P < 0.05$, Supplemental Fig. 2A).

ER stress inhibition after AMPK activation was also demonstrated after cardiac AC16 cells had been induced with tunicamycin, a mixture of homologous nucleoside antibiotics that acts as a potent pharmacologic ER-stress inducer. Tunicamycin elicited a huge increase in *sXBP1*, *ATF3* (3-fold, $P < 0.001$), *BiP/GRP78* (8-fold, $P < 0.001$) and *CHOP* (11-fold, $P < 0.001$) expression, as well as IRE-1α phosphorylation (2.5-fold, $P < 0.05$) (Fig. 4A). Co-incubation of tunicamycin-treated cells with AICAR prevented the rise of some of these ER stress markers, such as *BiP/GRP78* and *CHOP* expression, but not all (*sXBP1* and *ATF3*). Western-blot analyses revealed that AICAR also abolished the increase in CHOP protein induced by tunicamycin, as observed by mRNA levels, but not eIF2α or IRE-1α phosphorylation (Fig. 4B). Activation of AMPK by AICAR was again monitored by determination of ACC2 phosphorylation (Supplemental Fig. 2B).

Therefore, given that GW501516 can induce AMPK phosphorylation at Thr172 independently of PPARβ/δ activation, and we had observed that AMPK activation prevented palmitate-induced ER stress, we next examined whether this kinase was involved in the effects of GW501516. However, we found that compound C did not prevent GW501516-mediated effects on any of the ER stress markers examined (*ATF3*, *BiP/GRP78* and *CHOP* expression, Supplemental Fig. 3A). This indicates that AMPK did not mediate the beneficial effects of GW501516 on ER stress, and may be explained by the fact that , in contrast to previously reported data [27], GW501516 did not enhance AMPK and ACC2 phosphorylation in AC16 cells (Supplemental Fig. 3B). Likewise, GW501516 did not prevent either the effects of tunicamycin on the expression of *sXBP1*, *BiP/GRP78* and *CHOP*, or the phosphorylation of IRE-1α

(Supplemental Fig. 4). Overall, this reinforces the notion that the effects of GW501516 are not dependant on AMPK activation.

3.3. ER stress induced by an HFD in the heart of mice is exacerbated in PPARβ/δ knockout mice

To corroborate the results obtained with cultured human cardiac cells, we also conducted in vivo studies with mice fed an HFD rich in saturated fatty acids. Consistent with the in vitro studies, an HFD significantly induced *BiP/GRP78* and *CHOP* expression in the heart of male wild type mice (1.5-fold, $P < 0.001$, and 1.5-fold, $P < 0.01$, respectively, vs. wild type control diet) (Fig. 5A). To further confirm the protective role of PPARβ/δ, we took advantage of PPARβ/δ knockout mice. Interestingly, *BiP/GRP78* (1.5-fold, $P < 0.01$ vs. wild type mice) and *CHOP* (1.5-fold, $P < 0.05$) expression was also higher in PPARβ/δ knockout mice than in wild type mice (Fig. 5A). This indicates that PPARβ/δ somehow prevented ER stress in the heart of these mice. Western-blot analysis revealed that PPARβ/δ suppression also enhanced IRE-1α phosphorylation (2.5-fold, $P < 0.01$) (Fig. 5B), although no splicing of *XBP1* was detected (Supplemental Fig. 5A). All these changes coincided with diminished AMPK and ACC2 activity, as revealed by Western-blot (Supplemental Fig. 5B). This suggests that there was reduced fatty acid β-oxidation in mice fed an HFD and in PPARβ/δ knockout mice.

3.4. PPARβ/δ activity regulates autophagy in cardiac cells

As reported above, when ER stress becomes chronically activated, apoptosis is induced to remove affected cells. Therefore, the next goal of this study was to evaluate the presence of apoptosis in human cardiac cells treated with palmitate. This was attained by determining different apoptotic markers that are essential for the elimination of irreversibly damaged cells under chronic ER stress, such as α-spectrin breakdown and Bcl-2 protein levels, by means of Western-blot analysis, or *Bax*, *Bim* and *Puma* mRNA levels by real-time RT-PCR. As observed in Supplemental Fig. 6, 0.25 mM palmitate treatment for 18 h did not induce apoptosis in human cardiac AC16 cells. GW501516 did not display any effect on apoptosis, except for a slight but interesting decrease of *Bim* expression after co-incubation with palmitate (40% reduction, $P < 0.01$ vs. palmitate-treated cells).

After that, we examined the occurrence of autophagy in human cardiac cells by checking two well-established autophagic markers in eukaryotes, the LC3-II/LC3-I ratio and the protein levels of beclin-1,

which are both required for the formation of the autophagosome during autophagy. LC3 is considered a marker for autophagy when it is proteolytically processed to form LC3-II. In spite of beclin-1 and LC3 expression (Supplemental Fig. 7A) and the fact that protein levels (Fig. 6A) were not modified in palmitate-treated cells, we found that GW501516, alone or in combination with palmitate, significantly enhanced both markers of autophagy, beclin-1 (1.5-fold, $P < 0.05$) and the LC3-II/LC3-I ratio (1.75-fold, $P < 0.01$, Fig. 6A). GW501516 also induced autophagy in the presence of tunicamycin, which indicates that its effect was not dependent on the type of ER stress inducer (Supplemental Fig. 7B). On the contrary, autophagy was not observed after treatment with AICAR (Supplemental Fig. 7C). These results suggest that GW501516 induces autophagy by post-transcriptional mechanisms, and in an AMPK-independent manner. To further corroborate the effect of GW501516 on autophagy, we next incubated human cardiac cells with thapsigargin. Thapsigargin is a sesquiterpene lactone that is experimentally used to specifically inhibit the last step in the autophagic process, which also raises cytosolic calcium concentration, thereby inducing ER-stress. As shown in Fig. 6B, thapsigargin down-regulated the protein levels of beclin-1 (45% reduction, $P < 0.01$ vs. control cells) and the LC3-II/LC3-I ratio (35% reduction, $P < 0.05$), a fact which was not only prevented, but also further increased, after GW501516 co-incubation. Besides inhibiting autophagy, thapsigargin triggers expression of *CHOP*, a transcription factor involved in ER stress-induced apoptosis [10,28]. In accordance with this, we found that thapsigargin up-regulated BiP/GRP78 (3.5-fold, $P < 0.01$) and CHOP protein levels (7.5-fold, $P < 0.001$). The PPARβ/δ agonist GW501516 did not prevent the increase in BiP/GRP78 protein levels, but did attenuate those of CHOP (Supplemental Fig. 8), which suggests that this drug also down-regulated the ER stress induced by thapsigargin. Last, but not least, we demonstrated that HFD feeding or PPARβ/δ suppression clearly down-regulated beclin-1 and the LC3-II/LC3-I ratio in the heart of mice (Fig. 6C), which indicates that this nuclear receptor plays a key role in the control of the autophagic process in cardiac cells.

4. Discussion

In recent years, activation of the UPR during ER stress has evolved as a new mechanism involved in the association between saturated free fatty acid-induced inflammation and chronic metabolic diseases, such as obesity, insulin resistance, and type 2 diabetes [6,29]. Studies performed in muscle [4,30] and

pancreatic β-cells [28] have demonstrated that palmitate induces the splicing of *XBP1* and enhances the expression of ER stress markers such as *ATF3*, *BiP/GRP78* and *CHOP*, as well as the phosphorylation of IRE-1α [4,30]. In agreement with this, we report that palmitate induces *XBP1* splicing and IRE-1α phosphorylation, as well as ATF3, BiP/GRP78 and CHOP gene expression and protein accumulation in human cardiac cells. However, and in contrast to muscle cells [4,5,31], the PERK/eIF2α branch of the UPR pathway was not activated in human cardiac cells, since eIF2α phosphorylation at Ser51 remained unaltered after palmitate treatment. In addition, we demonstrate here for the first time in cardiac cells that PPARβ/δ activation with GW501516 prevents saturated fatty acid-induced ER stress, since it abolishes the rise in ATF3 and CHOP levels. Strikingly, GW501516 prevented IRE-1α phosphorylation, but this was not accompanied by *sXBP1* downregulation. This suggests that in human cardiac cells *XBP1* splicing depends on the action of a yet to uncover endoribonuclease or that the time chosen for analyses was too short. sXBP1 up-regulates many essential UPR genes involved in folding, organelle biogenesis, ERAD, autophagy, and protein quality control, but its specific target genes may vary depending on the cell type and the nature of the stressor stimulus [8]. Although *BiP/GRP78* expression may be transcriptionally controlled by the three UPR branches, and given that the effects of GW501516 on *XBP1* splicing fairly correlated with those of *BiP/GRP78* expression, our results suggest that, at least in human cardiac cells, *BiP/GRP78* might be transcriptionally controlled by sXBP1.

Owing to its high fat content, the Western-type diet is known to cause insulin resistance and type 2 diabetes mellitus, besides inducing ER stress and inflammation [30,32]. Our studies conducted in vivo with mice also demonstrate that saturated fatty acid-rich HFD feeding induces *BiP/GRP78* and *CHOP* expression in the heart. More importantly, the expression of these ER stress markers was also enhanced in PPARβ/δ knockout mice, thus indicating that PPARβ/δ somehow prevented ER stress in the heart of mice. In agreement to what happened in vitro, PPARβ/δ suppression enhanced IRE-1α phosphorylation, but not *XBP1* splicing. Unlike human cardiac cells in vitro, we found that eIF2α phosphorylation was enhanced in the heart of mice fed an HFD and also in PPARβ/δ knockout mice (Supplemental Fig. 9).

AMPK activation brings about multiple protective effects, including inhibition of inflammation, oxidative stress and insulin resistance, which result in a diminution of the risk for developing obesity and type 2

diabetes [33]. Recently, it has been reported that AMPK protects against cardiomyocyte hypoxic injury [34] and atherosclerosis [35] by reducing ER stress. When we examined the potential mechanisms responsible for the increase in ER stress following palmitate exposure, we observed that this saturated fatty acid reduced AMPK activity. In consonance with this, AICAR prevented the rise of most palmitate-induced ER stress markers. Similar results were obtained after induction of ER stress with tunicamycin. In contrast, our results clearly indicate that the preventive effects of GW501516 on palmitate- and tunicamycin-induced ER stress are AMPK-independent. On the contrary, results obtained in both mice fed an HFD and in PPARβ/δ knockout mice suggest that reduced fatty acid β-oxidation occurs in the heart. Nevertheless, our in vivo results match with those obtained in the liver and muscle of rodents after HFD feeding, in which saturated fatty acids appear to contribute to AMPK inhibition [36].

Prolonged or severe ER stress during diabetic cardiomyopathy leads to apoptotic cell death of cardiomyocytes [14] and, because myocytes rarely proliferate in the adult heart, the loss of cardiomyocytes will compromise cardiac function. The initiation of the caspase cascade during intrinsic apoptosis is mediated by BH3-only domain proteins such as Bim (B-cell lymphoma-2 [Bcl-2]-like 11) and Puma (Bcl-2 binding component 3), which are responsible for transmitting death signals by either inhibiting the Bcl-2 anti-apoptotic members (Bcl-2; Bcl-xL, B-cell lymphoma-extra large) or activating the pro-apoptotic Bcl-2 multi-domain proteins (Bax, Bcl-2-associated X protein; Bak, Bcl-2 homologous antagonist/killer) at the mitochondria. The UPR promotes the expression of CHOP, a pro-apoptotic transcription factor that has a critical role in cardiac cell death caused by chronic ER stress during heart failure [11] and cardiac hypertrophy [37]. The UPR, possibly through CHOP, down-regulates the anti-apoptotic Bcl-2 family of proteins, but transcriptionally up-regulates Bim and Puma. Overall, this contributes to apoptosis in cells undergoing irreversible ER stress [8]. However, although we had found a significant increase in CHOP protein levels after palmitate treatment, no changes in any of the apoptotic markers examined were detected in human cardiac cells. In accordance with this, Quentin *et al*. [38] demonstrated that CHOP is not necessarily a mediator of apoptosis in rat cardiomyocytes. Nevertheless, our results contrast with those obtained in diverse hepatoma cell lines [39,40], in which palmitic acid was found to induce ER stress and subsequent apoptosis. Although GW501516 prevented the rise in CHOP protein levels after palmitate treatment in human cardiac cells, it did not reduce apoptosis. The relatively

short duration of palmitate treatment might account for the lack of apoptotic activation in human cardiac cells, since several authors have speculated that the transition between adaptive UPR and apoptosis depends, at least in part, on the duration of ER stress stimulation [8].

It is widely accepted that, when ER stress is limited, the UPR potentiates autophagy as a short-term strategy to protect cells. Thus, suppression of autophagy favours the development of heart failure during diabetes [41], whereas its induction may reduce myocardial ischemia/reperfusion-induced lethal injury [10]. The most striking result of our study is the enhancement of two well-known markers of autophagy in cardiac cells after GW501516 treatment and in the heart of mice fed an HFD. More importantly, we also report here that PPARβ/δ suppression down-regulates autophagic markers in the heart of mice, hence suggesting that this nuclear receptor is crucial in regulating the autophagic process in cardiac cells. However, and unlike a previous study performed with rat heart [10], we did not find any correlation between eIF2α phosphorylation and the conversion of LC3-II from LC3-I. This suggests that the PERK/eIF2α pathway is not essential for autophagy in our model. In fact, our results better fit with those obtained by Ogata *et al*. [42] in mouse embryonic fibroblasts, which demonstrated that activation of autophagy by ER stress depends on the kinase domain of IRE-1α, but not on its endoribonuclease activity on *XBP1* nor on the PERK/eIF2α pathway. A recent study demonstrated that activation of AMPK restores cardiac autophagy and protects against cardiac cell apoptosis, which ultimately improves cardiac function in diabetic mice [41]. In contrast, our results indicate that GW501516 induces autophagy by post-transcriptional mechanisms in an AMPK-independent manner. This discrepancy might be explained by the fact that He and collaborators investigated autophagy in the context of high glucose conditions, and AMPK is a well-recognized regulator of glucose homeostasis. However, recent studies performed in mice fed an HFD reported that autophagy is down-regulated in adipose tissue [43] and in the heart [44]. The former study also demonstrates that autophagy suppression induces inflammatory responses via ER stress activation, while the opposite, that is activation of autophagy with rapamycin, decreases inflammatory gene expression [43]. Overall, and taking into account our previous data demonstrating that PPARβ/δ can limit myocardial inflammation by NF-κB inhibition [15], we hypothesize that GW501516 might prevent ER stress in human cardiac cells by means of autophagy activation. This is supported by

our results demonstrating that the NF-κB inhibitor parthenolide prevented the up-regulation of *ATF3* and *CHOP* expression induced by palmitate in human cardiac cells (Supplemental Fig. 10).

Given its causative role in cardiovascular diseases associated with metabolic disorders such as obesity and diabetes, ER stress has been suggested as a useful therapeutic target. With this aim, several chemical chaperones have been examined in a number of disease models as potential tools for preventing ER stress and the activation of the UPR, since they play a similar role to endogenous chaperones, stabilizing proteins and assisting in their proper folding [45]. For instance, 4-phenylbutyric acid (PBA) and tauroursodeoxycholic acid (TUDCA) have had beneficial effects on insulin resistance, obesity and diabetes in several in vitro [4,5] and in vivo [46] models. However, chemical chaperones have major drawbacks: their null specificity and a high-dose is required to obtain effective protein folding properties. Therefore, the research and development of new drugs that target ER stress during metabolic diseases without the undesired effects of chemical chaperones is of great interest.

5. Study limitations

A major drawback of the study might be the origin of the AC16 cell line itself, since it consists of a fusion of primary ventricular cells with SV-40-transformed fibroblasts. However, this cell line develops many of the biochemical and morphological properties characteristic of cardiac muscle cells, even though it does not form completely differentiated cardiomyocytes [47]. Furthermore, the more relevant findings obtained in this study with AC16 human cardiac cells have been further corroborated later in the heart of mice.

6. Conclusions

Results herein reported demonstrate that PPARβ/δ activation with GW501516 attenuates palmitate-induced ER stress and induces autophagy in human cardiac cells (Figure 7), thereby adding a new beneficial mechanism for this drug. In this context, activation of autophagy has already been suggested as a useful therapeutic approach for diabetes, owing to its ability to reduce ER stress in pancreatic β-cells [48]. PPARβ/δ has many valuable physiological functions ranging from enhanced fatty acid catabolism and improved insulin sensitivity, to inflammation inhibition, thus displaying a potential therapeutic role for the prevention and treatment of diseases including diabetes, dyslipidemias or metabolic syndrome.

Since chronic low-grade inflammation and ER stress play a significant role in cardiac hypertrophy and heart failure, and GW501516 has been shown to ameliorate metabolic disturbances in heart caused by high-fat diets [15], it is tempting to speculate that PPARβ/δ might serve as a therapeutic target to prevent cardiac hypertrophy and heart failure induced by ER stress during metabolic disorders.

Glossary: ACC, acetyl-CoA carboxylase; ACO, acyl-CoA oxidase; AICAR, 5-aminoimidazole-4-carboxamide ribonucleotide; AMPK, 5' AMP-activated protein kinase; ATF, activating transcription factor; Bax, Bcl-2-associated X protein; Bcl-2, B-cell lymphoma 2; Bim, Bcl-2-like 11; BiP/GRP78, binding immunoglobulin protein/glucose-regulated protein; CHOP, CCAAT/enhancer binding protein (C/EBP) homologous protein; CPT-1b, carnitine palmitoyltransferase 1b; ER, endoplasmic reticulum; ERAD, ER-associated degradation; HFD, high-fat diet; IRE-1α, inositol-requiring enzyme-1α; LC3, microtubule-associated protein 1A/1B-light chain 3; NF-κB, nuclear factor-κB; PERK, PKR-like ER kinase; PPARβ/δ, peroxisome proliferator-activated receptor β/δ; Puma, Bcl-2 binding component 3; UPR, unfolded protein response; XBP1, X-box binding protein 1

Appendix A. Supplementary data

Supplementary data to this article can be found online.

References

[1] Diakogiannaki E, Welters HJ, Morgan NG. Differential regulation of the endoplasmic reticulum stress response in pancreatic beta-cells exposed to long-chain saturated and monounsaturated fatty acids. J Endocrinol 2008;197:553-63.

[2] Karaskov E, Scott C, Zhang L, Teodoro T, Ravazzola M, Volchuk A. Chronic palmitate but not oleate exposure induces endoplasmic reticulum stress, which may contribute to INS-1 pancreatic beta-cell apoptosis. Endocrinology 2006;147:3398-407.

[3] Jung TW, Lee KT, Lee MW, Ka KH. SIRT1 attenuates palmitate-induced endoplasmic reticulum stress and insulin resistance in HepG2 cells via induction of oxygen-regulated protein 150. Biochem Biophys Res Commun 2012;422:229-32.

[4] Salvadó L, Coll T, Gomez-Foix AM, et al. Oleate prevents saturated-fatty-acid-induced ER stress, inflammation and insulin resistance in skeletal muscle cells through an AMPK-dependent mechanism. Diabetologia 2013;56:1372-82.

[5] Peng G, Li L, Liu Y, et al. Oleate blocks palmitate-induced abnormal lipid distribution, endoplasmic reticulum expansion and stress, and insulin resistance in skeletal muscle. Endocrinology 2011;152:2206-18.

[6] Hotamisligil GS. Endoplasmic reticulum stress and the inflammatory basis of metabolic disease. Cell 2010;140:900-17.

[7] Xu J, Zhou Q, Xu W, Cai L. Endoplasmic reticulum stress and diabetic cardiomyopathy. Exp Diabetes Res 2012;2012:827971.

[8] Hetz C, Martinon F, Rodriguez D, Glimcher LH. The Unfolded Protein Response: Integrating Stress Signals Through the Stress Sensor IRE1{alpha}. Physiol Rev 2011;91:1219-43.

[9] Ma Y, Brewer JW, Diehl JA, Hendershot LM. Two distinct stress signaling pathways converge upon the CHOP promoter during the mammalian unfolded protein response. J Mol Biol 2002;318:1351-65.

[10] Petrovski G, Das S, Juhasz B, Kertesz A, Tosaki A, Das DK. Cardioprotection by endoplasmic reticulum stress-induced autophagy. Antioxid Redox Signal 2011;14:2191-200.

[11] Zhao H, Liao Y, Minamino T, et al. Inhibition of cardiac remodeling by pravastatin is associated with amelioration of endoplasmic reticulum stress. Hypertens Res 2008;31:1977-87.

[12] Li Z, Zhang T, Dai H, et al. Involvement of endoplasmic reticulum stress in myocardial apoptosis of streptozocin-induced diabetic rats. J Clin Biochem Nutr 2007;41:58-67.

[13] Lakshmanan AP, Meilei H, Suzuki K, et al. The hyperglycemia stimulated myocardial endoplasmic reticulum (ER) stress contributes to diabetic cardiomyopathy in the transgenic non-obese type 2 diabetic rats: A differential role of Unfolded Protein Response (UPR) signaling proteins. Int J Biochem Cell Biol 2012;45:438-47.

[14] Takada A, Miki T, Kuno A, et al. Role of ER stress in ventricular contractile dysfunction in type 2 diabetes. PLoS One 2012;7:e39893.

[15] Álvarez-Guardia D, Palomer X, Coll T, et al. PPARbeta/delta activation blocks lipid-induced inflammatory pathways in mouse heart and human cardiac cells. Biochim Biophys Acta 2011;1811:59-67.

[16] Hamid T, Guo SZ, Kingery JR, Xiang X, Dawn B, Prabhu SD. Cardiomyocyte NF-kappaB p65 promotes adverse remodelling, apoptosis, and endoplasmic reticulum stress in heart failure. Cardiovasc Res 2011;89:129-38.

[17] Cheng L, Ding G, Qin Q, et al. Cardiomyocyte-restricted peroxisome proliferator-activated receptor-delta deletion perturbs myocardial fatty acid oxidation and leads to cardiomyopathy. Nat Med 2004;10:1245-50.

[18] Wang P, Liu J, Li Y, et al. Peroxisome proliferator-activated receptor {delta} is an essential transcriptional regulator for mitochondrial protection and biogenesis in adult heart. Circ Res 2010;106:911-9.

[19] Cao M, Tong Y, Lv Q, et al. PPARdelta Activation Rescues Pancreatic beta-Cell Line INS-1E from Palmitate-Induced Endoplasmic Reticulum Stress through Enhanced Fatty Acid Oxidation. PPAR Res 2012;2012:680684.

[20] Ramirez T, Tong M, Chen WC, Nguyen QG, Wands JR, de la Monte SM. Chronic alcohol-induced hepatic insulin resistance and ER stress ameliorated by PPAR-delta agonist treatment. J Gastroenterol Hepatol 2013;28:179-87.

[21] Palomer X, Álvarez-Guardia D, Rodriguez-Calvo R, et al. TNF-alpha reduces PGC-1alpha expression through NF-kappaB and p38 MAPK leading to increased glucose oxidation in a human cardiac cell model. Cardiovasc Res 2009;81:703-12.

[22] Coll T, Palomer X, Blanco-Vaca F, et al. Cyclooxygenase 2 Inhibition Exacerbates Palmitate-Induced Inflammation and Insulin Resistance in Skeletal Muscle Cells. Endocrinology 2010;151:537-48.

[23] Nadra K, Anghel SI, Joye E, et al. Differentiation of trophoblast giant cells and their metabolic functions are dependent on peroxisome proliferator-activated receptor beta/delta. Mol Cell Biol 2006;26:3266-81.

[24] Palomer X, Capdevila-Busquets E, Álvarez-Guardia D, et al. Resveratrol induces nuclear factor-kappaB activity in human cardiac cells. Int J Cardiol 2013;167:2507-16.

[25] Bradford MM. A rapid and sensitive method for the quantitation of microgram quantities of protein utilizing the principle of protein-dye binding. Anal Biochem 1976;72:248-54.

[26] Álvarez-Guardia D, Palomer X, Coll T, et al. The p65 subunit of NF-kappaB binds to PGC-1alpha, linking inflammation and metabolic disturbances in cardiac cells. Cardiovasc Res 2010;87:449-58.

[27] Kramer DK, Al Khalili L, Guigas B, Leng Y, Garcia-Roves PM, Krook A. Role of AMP kinase and PPARdelta in the regulation of lipid and glucose metabolism in human skeletal muscle. J Biol Chem 2007;282:19313-20.

[28] Kharroubi I, Ladriere L, Cardozo AK, Dogusan Z, Cnop M, Eizirik DL. Free fatty acids and cytokines induce pancreatic beta-cell apoptosis by different mechanisms: role of nuclear factor-kappaB and endoplasmic reticulum stress. Endocrinology 2004;145:5087-96.

[29] Zhang K, Kaufman RJ. From endoplasmic-reticulum stress to the inflammatory response. Nature 2008;454:455-62.

[30] Rieusset J, Chauvin MA, Durand A, et al. Reduction of endoplasmic reticulum stress using chemical chaperones or Grp78 overexpression does not protect muscle cells from palmitate-induced insulin resistance. Biochem Biophys Res Commun 2011;417:439-45.

[31] Hage Hassan R., Hainault I, Vilquin JT, et al. Endoplasmic reticulum stress does not mediate palmitate-induced insulin resistance in mouse and human muscle cells. Diabetologia 2012;55:204-14.

[32] Panzhinskiy E, Hua Y, Culver B, Ren J, Nair S. Endoplasmic reticulum stress upregulates protein tyrosine phosphatase 1B and impairs glucose uptake in cultured myotubes. Diabetologia 2012;56:598-607.

[33] Shaw RJ, Lamia KA, Vasquez D, et al. The kinase LKB1 mediates glucose homeostasis in liver and therapeutic effects of metformin. Science 2005;310:1642-6.

[34] Yeh CH, Chen TP, Wang YC, Lin YM, Fang SW. AMP-activated protein kinase activation during cardioplegia-induced hypoxia/reoxygenation injury attenuates cardiomyocytic apoptosis via reduction of endoplasmic reticulum stress. Mediators Inflamm 2010;2010:130636.

[35] Dong Y, Zhang M, Liang B, et al. Reduction of AMP-activated protein kinase alpha2 increases endoplasmic reticulum stress and atherosclerosis in vivo. Circulation 2010;121:792-803.

[36] Muse ED, Obici S, Bhanot S, et al. Role of resistin in diet-induced hepatic insulin resistance. J Clin Invest 2004;114:232-9.

[37] Ni L, Zhou C, Duan Q, et al. beta-AR Blockers Suppresses ER Stress in Cardiac Hypertrophy and Heart Failure. PLoS One 2011;6:e27294.

[38] Quentin T, Steinmetz M, Poppe A, Thoms S. Metformin differentially activates ER stress signaling pathways without inducing apoptosis. Dis Model Mech 2011;5:259-69.

[39] Zhang Y, Xue R, Zhang Z, Yang X, Shi H. Palmitic and linoleic acids induce ER stress and apoptosis in hepatoma cells. Lipids Health Dis 2012;11:1.

[40] Cao J, Dai DL, Yao L, et al. Saturated fatty acid induction of endoplasmic reticulum stress and apoptosis in human liver cells via the PERK/ATF4/CHOP signaling pathway. Mol Cell Biochem 2012;364:115-29.

[41] He C, Zhu H, Li H, Zou MH, Xie Z. Dissociation of Bcl-2-Beclin1 Complex by Activated AMPK Enhances Cardiac Autophagy and Protects Against Cardiomyocyte Apoptosis in Diabetes. Diabetes 2012;62:1270-81.

[42] Ogata M, Hino S, Saito A, et al. Autophagy is activated for cell survival after endoplasmic reticulum stress. Mol Cell Biol 2006;26:9220-31.

[43] Yoshizaki T, Kusunoki C, Kondo M, et al. Autophagy regulates inflammation in adipocytes. Biochem Biophys Res Commun 2012;417:352-7.

[44] Guo R, Zhang Y, Turdi S, Ren J. Adiponectin knockout accentuates high fat diet-induced obesity and cardiac dysfunction: Role of autophagy. Biochim Biophys Acta 2013;1832:1136-48.

[45] Basseri S, Austin RC. Endoplasmic reticulum stress and lipid metabolism: mechanisms and therapeutic potential. Biochem Res Int 2012;2012:841362.

[46] Ozcan U, Yilmaz E, Ozcan L, et al. Chemical chaperones reduce ER stress and restore glucose homeostasis in a mouse model of type 2 diabetes. Science 2006;313:1137-40.

[47] Davidson MM, Nesti C, Palenzuela L, et al. Novel cell lines derived from adult human ventricular cardiomyocytes. J Mol Cell Cardiol 2005;39:133-47.

[48] Bachar-Wikstrom E, Wikstrom JD, Ariav Y, et al. Stimulation of Autophagy Improves Endoplasmic Reticulum Stress-Induced Diabetes. Diabetes 2012;62:1227-37.

Fig. 1. Palmitate induces endoplasmic reticulum stress markers in human cardiac cells. *sXBP1*, *ATF3*, *BiP/GRP78* and *CHOP* mRNA levels in AC16 cells incubated for 18 h with palmitate (Pal, 0.25 mmol/L). The graphs represent the quantification of the *18S*-normalized mRNA levels, expressed as a percentage of control samples ±SD. ***$P < 0.001$ vs. Control (Ctrl).

Fig. 2. PPARβ/δ activation prevents palmitate-induced ER stress in human cardiac cells. AC16 cells were incubated for 18 h with palmitate (Pal, 0.25 mmol/L) in the presence or absence of GW501516 (GW, 10 μmol/L) or GSK0660 (GSK, 10 μmol/L). (A) *sXBP1*, *ATF3*, *BiP/GRP78* and *CHOP* mRNA levels. The graphs represent the quantification of the *18S*-normalized mRNA levels, expressed as a percentage of control samples ±SD. (B) Western-blot analysis showing protein levels of BiP/GRP78, CHOP and the ratio phosphorylated IRE-1α^{Ser724}/IRE-1α in total protein extracts. To show equal loading of protein, the actin signal is included from the same blot. The graphs represent the quantification of the normalized protein levels expressed as a percentage of control samples ±SD. All autoradiograph data are representative of two separate experiments. *$P < 0.05$, **$P < 0.01$ and ***$P < 0.001$ vs. Ctrl; †$P < 0.05$, ††$P < 0.01$ and ‡$P < 0.001$ vs. Pal; &$P < 0.05$ vs. Pal+GW.

Fig. 3. AMPK activation avoids palmitate-induced ER stress in human cardiac cells. AC16 cells were incubated for 18 h with palmitate (Pal, 0.25 mmol/L) in the presence or absence of AICAR (AIC, 2 mmol/L) or Compound C (CC, 30 μmol/L). (A) *sXBP1*, *ATF3*, *BiP/GRP78* and *CHOP* mRNA levels. The graphs represent the quantification of the *18S*-normalized mRNA levels, expressed as a percentage of control samples ±SD. (B) Western-blot analysis showing protein levels of BiP/GRP78, CHOP and the ratio phosphorylated IRE-1α^{Ser724}/IRE-1α in total protein extracts. To show equal loading of protein, the actin signal is included from the same blot. The graphs represent the quantification of the normalized protein levels expressed as a percentage of control samples ±SD. All autoradiograph data are representative of two separate experiments. *$P < 0.05$, **$P < 0.01$ and ***$P < 0.001$ vs. Ctrl; †$P < 0.05$, ††$P < 0.01$ and ‡$P < 0.001$ vs. Pal; #$P < 0.05$ and &$P < 0.01$ vs. Pal+AIC.

Fig. 4. Tunicamycin elicits ER stress in human cardiac cells. AC16 cells were incubated for 4 h with tunicamycin (Tun, 5 μg/mL) and AICAR (AIC, 2 mmol/L). (A) *sXBP1*, *ATF3*, *BiP/GRP78* and *CHOP* mRNA levels. The graphs represent the quantification of the *18S*-normalized mRNA levels, expressed as a percentage of control samples ±SD. (B) Western-blot analysis showing protein levels of CHOP, phosphorylated eIF2α^{Ser51}/eIF2α and phosphorylated IRE-1α^{Ser724}/IRE-1α in total protein extracts. To show equal loading of protein, the actin signal is included from the same blot. The graphs represent the quantification of the normalized protein levels expressed as a percentage of control samples ±SD. All autoradiograph data are representative of two separate experiments. **P* < 0.05, ***P* < 0.01 and ****P* < 0.001 vs. Ctrl; †*P* < 0.05, ††*P* < 0.01 and ‡*P* < 0.001 vs. Tun.

Fig. 5. ER stress induced by an HFD in the heart of mice is exacerbated in PPARβ/δ knockout mice. (A) Relative quantification of *BiP/GRP78* and *CHOP* mRNA levels assessed by real-time RT-PCR of samples obtained from the heart of wild-type (WT) or knockout PPARβ/δ (KO) mice fed a standard chow diet (Ctrl) or a saturated fatty acid-rich diet (HFD) for two months. The graphs represent the quantification of the *APRT*-normalized mRNA levels, expressed as a percentage of control samples ±SD. (B) Western-blot analysis showing the levels of phosphorylated IRE-1α^{Ser724}/IRE-1α in total protein extracts obtained from the samples depicted in panel A. The graphs represent the quantification of the normalized protein levels expressed as a percentage of control samples ±SD. All autoradiograph data are representative of two separate experiments. **P* < 0.05, ***P* < 0.01 and ****P* < 0.001 vs. WT Ctrl.

Fig. 6. PPARβ/δ activity regulates autophagy in cardiac cells. Western-blot analysis showing protein levels of beclin-1 and the LC3-II/LC3-I ratio in total protein extracts obtained from human cardiac AC16 cells incubated for (A) 18 h with palmitate (Pal, 0.25 mmol/L) or (B) 18 h with thapsigargin (Thap, 1 μmol/L), both in the presence or absence of GW501516 (GW, 10 μmol/L). (C) Western-blot analysis showing protein levels of beclin-1 and the LC3-II/LC3-I ratio in total protein extracts isolated from the heart of wild-type (WT) or knockout PPARβ/δ (KO) mice fed a standard chow diet (Ctrl) or a saturated fatty acid-rich diet (HFD) for two months. The graphs represent the quantification of the normalized

protein levels expressed as a percentage of control samples ±SD. All autoradiograph data are representative of two separate experiments. (A) and (B) *$P < 0.05$, **$P < 0.01$ and ***$P < 0.001$ vs. Ctrl; †$P < 0.05$ vs. Pal; &$P < 0.01$, #$P < 0.001$ vs. Thap. (C) *$P < 0.05$, **$P < 0.01$ and ***$P < 0.001$ vs. WT Ctrl.

Fig. 7. PPARβ/δ attenuates palmitate-induced endoplasmic reticulum stress and induces autophagy. Initiation of the UPR involves the activation of ATF6, IRE-1α and PERK pathways. In the absence of stress, these trans-membrane proteins are bound to the intra-luminal BiP/GRP78 protein. On stress exposure, the large excess of unfolded proteins sequesters BiP/GRP78 from trans-membrane ER proteins, thereby inducing the UPR. After proteolytically processing at the Golgi complex, ATF6 translocates to the nucleus, in which it acts as a transcription factor for ER chaperones and ERAD-related genes. On the other hand, the endoribonuclease activity of IRE-1α cleaves the mRNA of *XBP1*, creating an alternative message that is translated into the spliced and active form of this transcription factor (sXBP1). Active IRE-1α also regulates responses mediated by mitogen-activated protein kinases (MAPKs) and NF-κB, which are relevant factors for the induction of apoptosis and inflammatory processes by ER stress. Finally, PERK phosphorylates and inhibits eIF2α, and by this means inhibits the translation of most mRNAs. However, some mRNAs escape this translational control, for example transcription factor *ATF4* (and its target genes *ATF3*, *BiP/GRP78* and *CHOP*) and genes involved in autophagy and apoptosis. If ER stress is limited, the UPR will potentiate autophagy to protect the cells. However, if ER stress is prolonged, the UPR will turn on apoptosis for removing cells that threaten the integrity of the organism. Palmitate induces *XBP1* splicing and IRE-1α phosphorylation, as well as ATF3, BiP/GRP78 and CHOP gene expression and protein accumulation in human cardiac cells. PPARβ/δ activation with GW501516 prevents saturated fatty acid-induced ER stress, since it abolishes the rise in ATF3 and CHOP levels and prevents IRE-1α phosphorylation in palmitate-treated cells. **ATF**, activating transcription factor; **BiP/GRP78**, binding immunoglobulin protein/glucose-regulated protein 78; **CHOP**, CCAAT/enhancer binding protein homologous protein; **eIF2α**, eukaryotic initiation factor 2α; **ERAD**, ER-associated degradation; **IRE-1α**, inositol-requiring enzyme; **PERK**, PKR-like ER kinase.

Figure 1

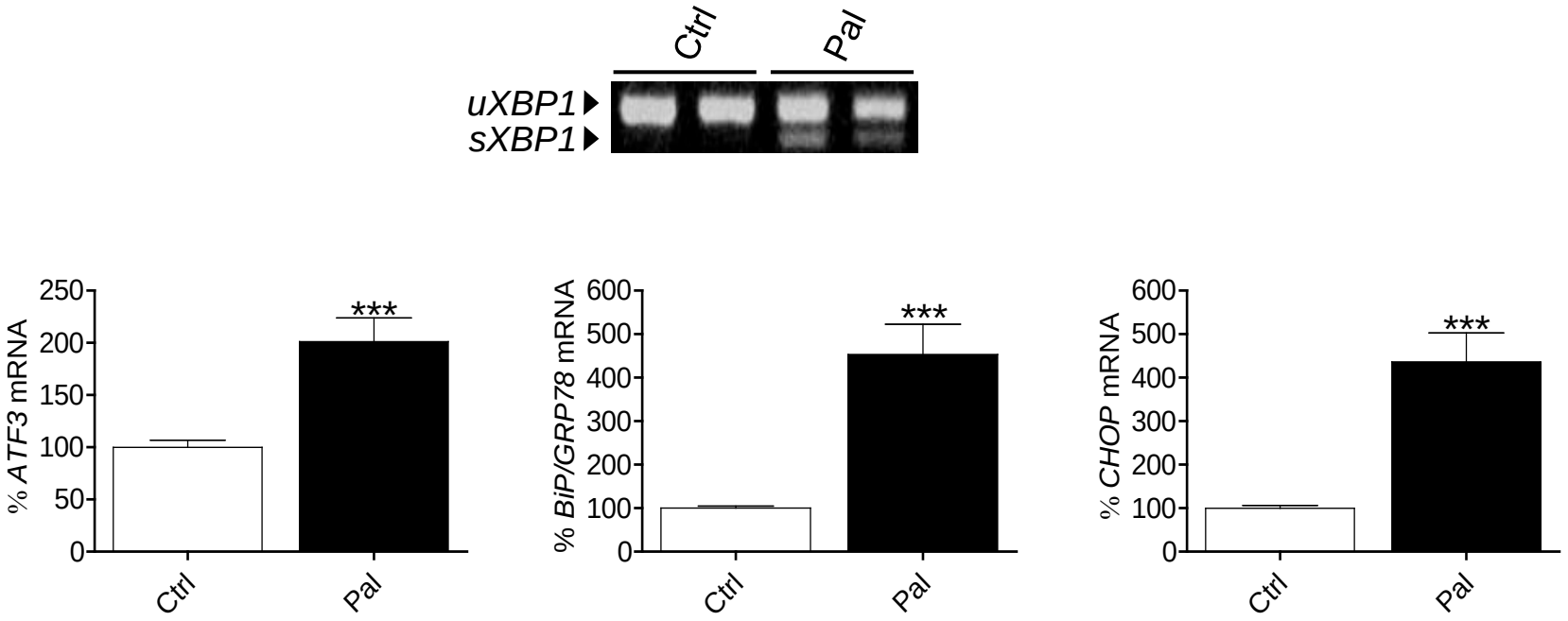
Ctrl
Pal
uXBP1
sXBP1
% ATF3 mRNA
250
200
150
100
50
0
***
Ctrl
Pal
% BiP/GRP78 mRNA
600
500
400
300
200
100
0
***
Ctrl
Pal
% CHOP mRNA
600
500
400
300
200
100
0
***
Ctrl
Pal

Figure 2

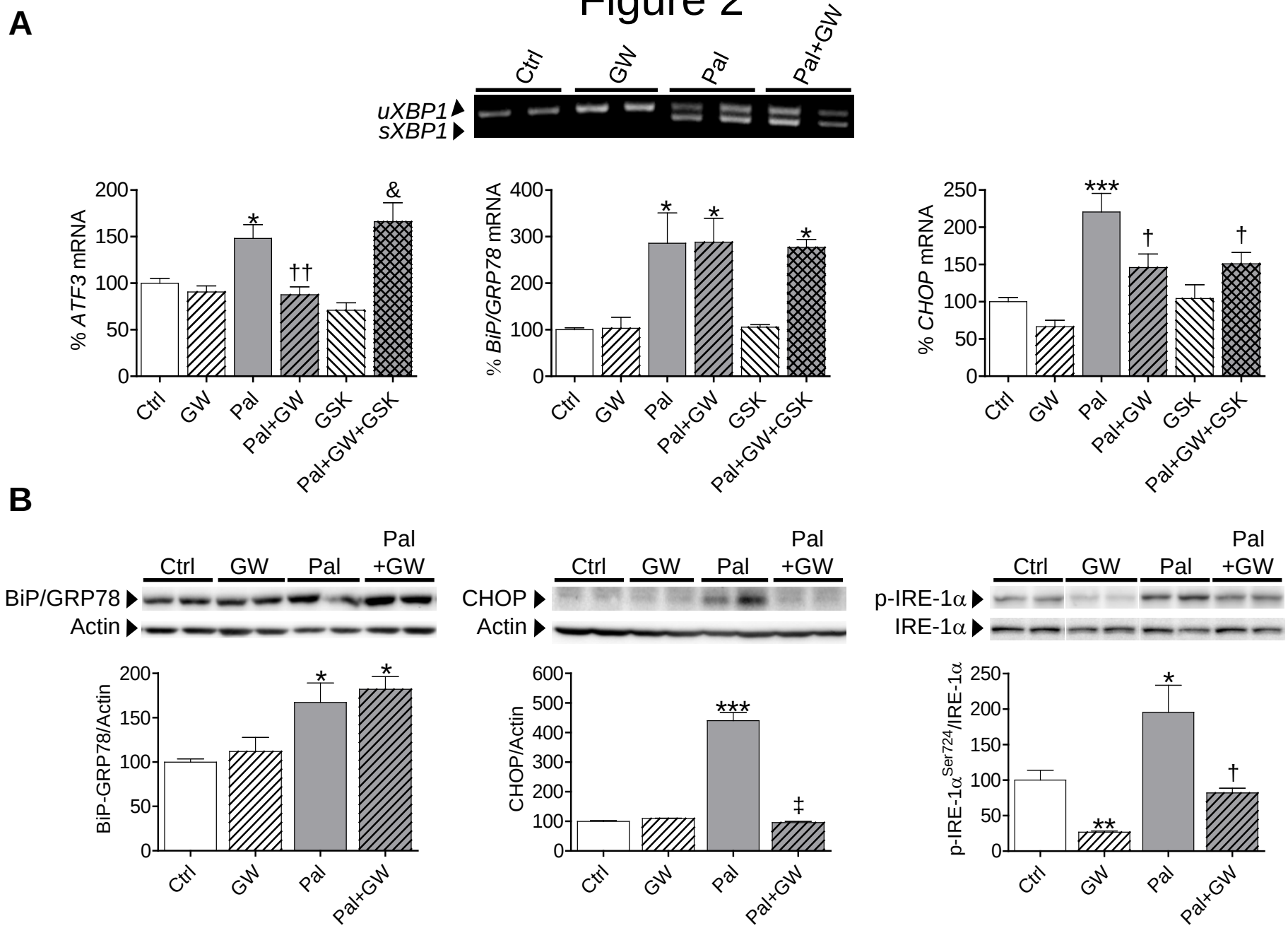
A
Ctrl
GW
Pal
Pal+GW
uXBP1
sXBP1
% ATF3 mRNA
% BiP/GRP78 mRNA
% CHOP mRNA
Ctrl
GW
Pal
Pal+GW
GSK
Pal+GW+GSK
B
BiP/GRP78
Actin
CHOP
p-IRE-1α
IRE-1α
BiP-GRP78/Actin
CHOP/Actin
p-IRE-1α Ser724/IRE-1α

Figure 3

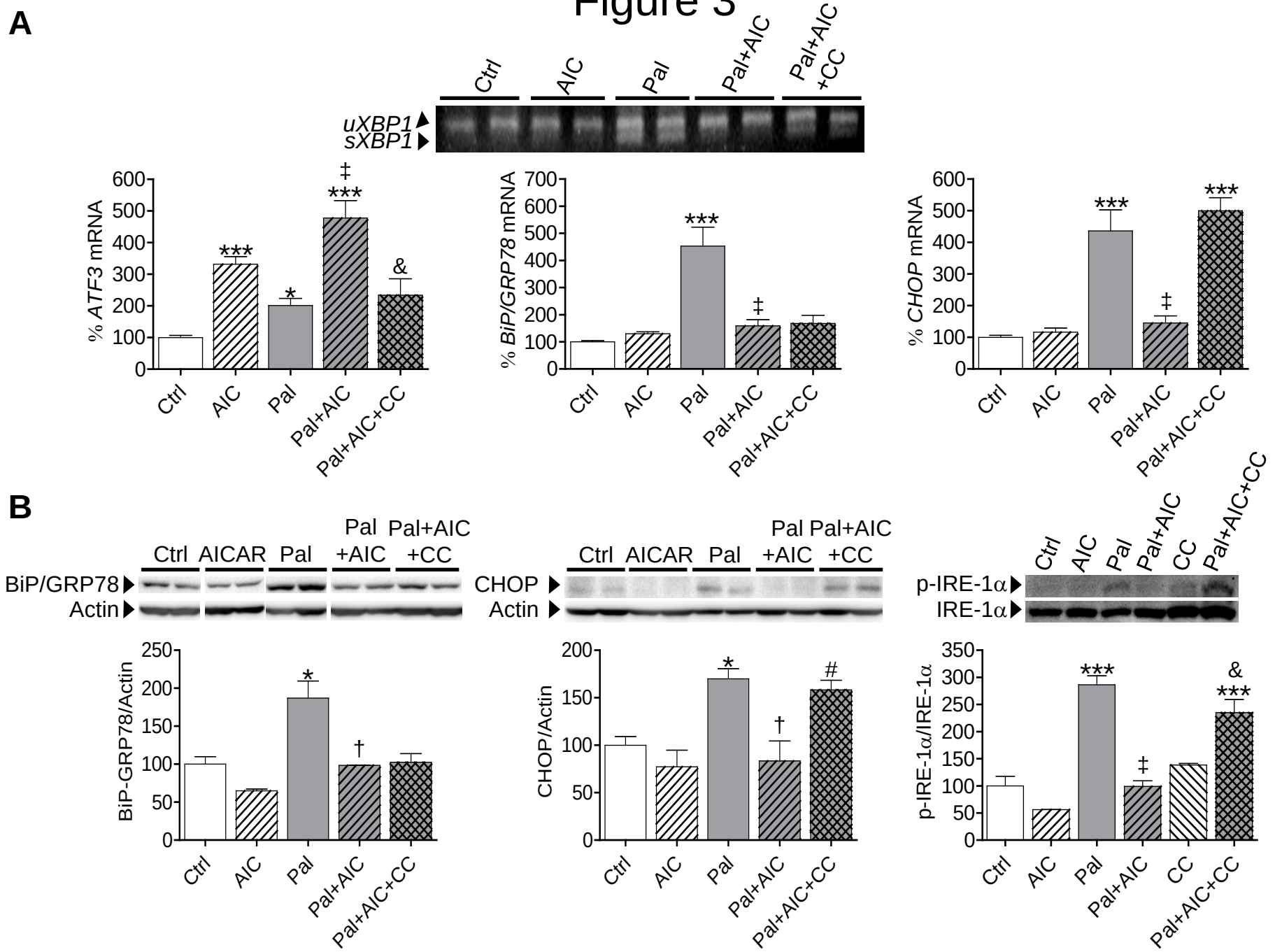
A
Ctrl
AIC
Pal
Pal+AIC
Pal+AIC +CC
uXBP1
sXBP1
% ATF3 mRNA
% BiP/GRP78 mRNA
% CHOP mRNA
Ctrl
AIC
Pal
Pal+AIC
Pal+AIC+CC
B
Ctrl AICAR Pal Pal +AIC Pal+AIC +CC
BiP/GRP78
Actin
CHOP
p-IRE-1α
IRE-1α
Ctrl AIC Pal Pal+AIC CC Pal+AIC+CC
BiP-GRP78/Actin
CHOP/Actin
p-IRE-1α/IRE-1α

Figure 4

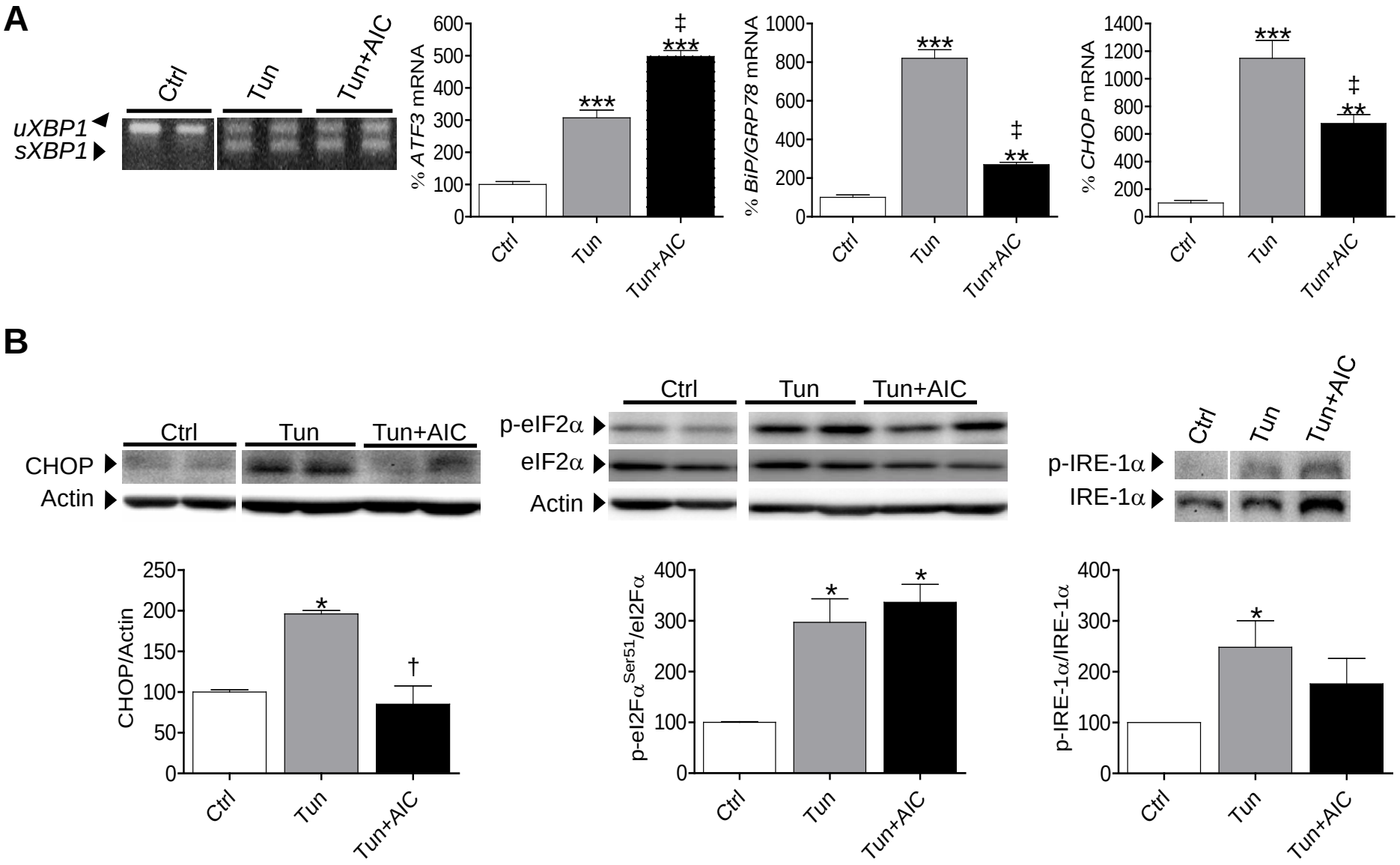
A
Ctrl
Tun
Tun+AIC
uXBP1
sXBP1
% ATF3 mRNA
% BiP/GRP78 mRNA
% CHOP mRNA
***
‡
**
B
CHOP
Actin
p-eIF2α
eIF2α
p-IRE-1α
IRE-1α
CHOP/Actin
p-eI2Fα Ser51/eI2Fα
p-IRE-1α/IRE-1α
*
†

Figure 5

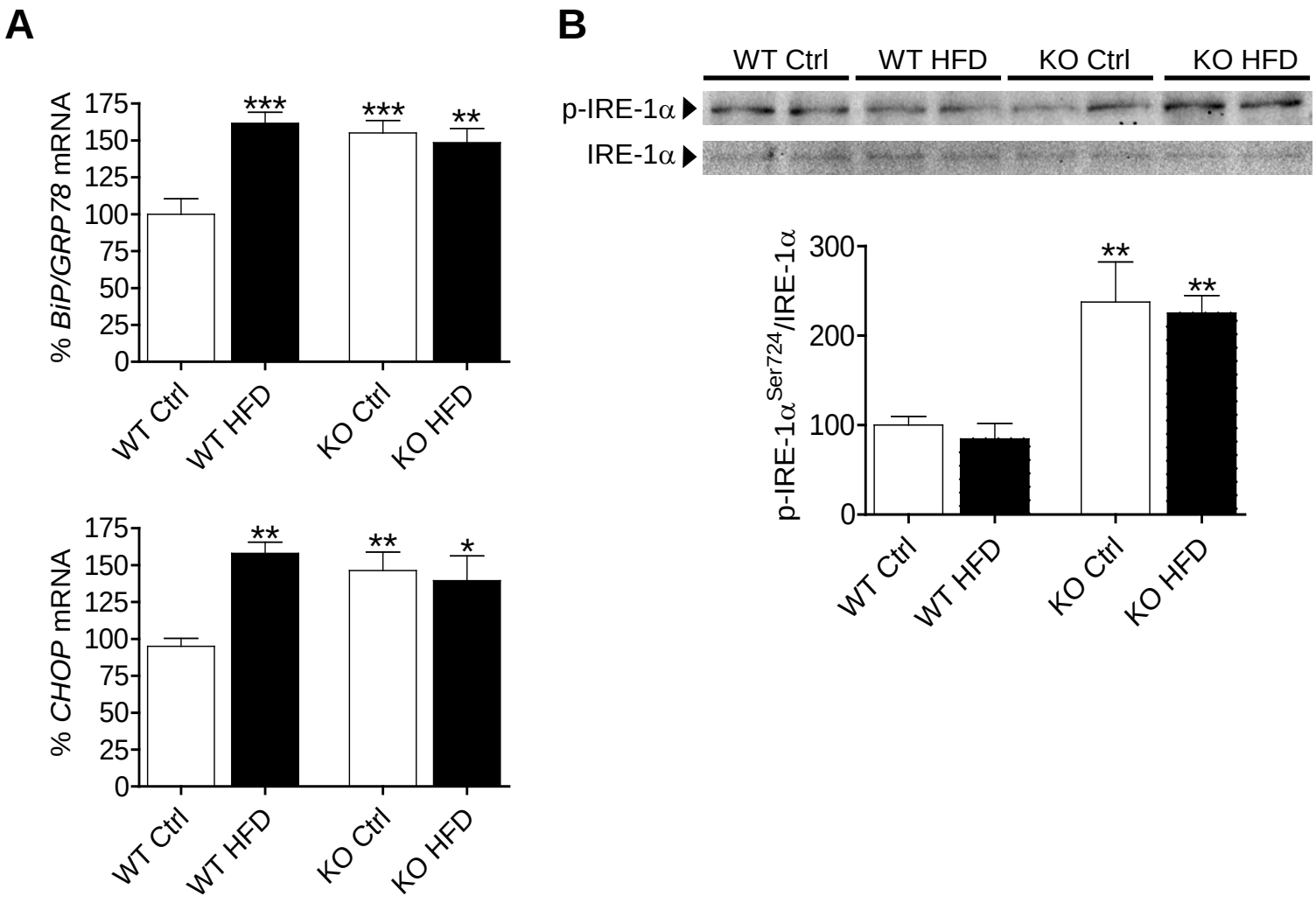
A
% BiP/GRP78 mRNA
175
150
125
100
75
50
25
0
***
***
**
WT Ctrl
WT HFD
KO Ctrl
KO HFD
% CHOP mRNA
175
150
125
100
75
50
25
0
**
**
*
WT Ctrl
WT HFD
KO Ctrl
KO HFD
B
WT Ctrl
WT HFD
KO Ctrl
KO HFD
p-IRE-1α
IRE-1α
p-IRE-1α Ser724/IRE-1α
300
200
100
0
**
**
WT Ctrl
WT HFD
KO Ctrl
KO HFD

Figure 6

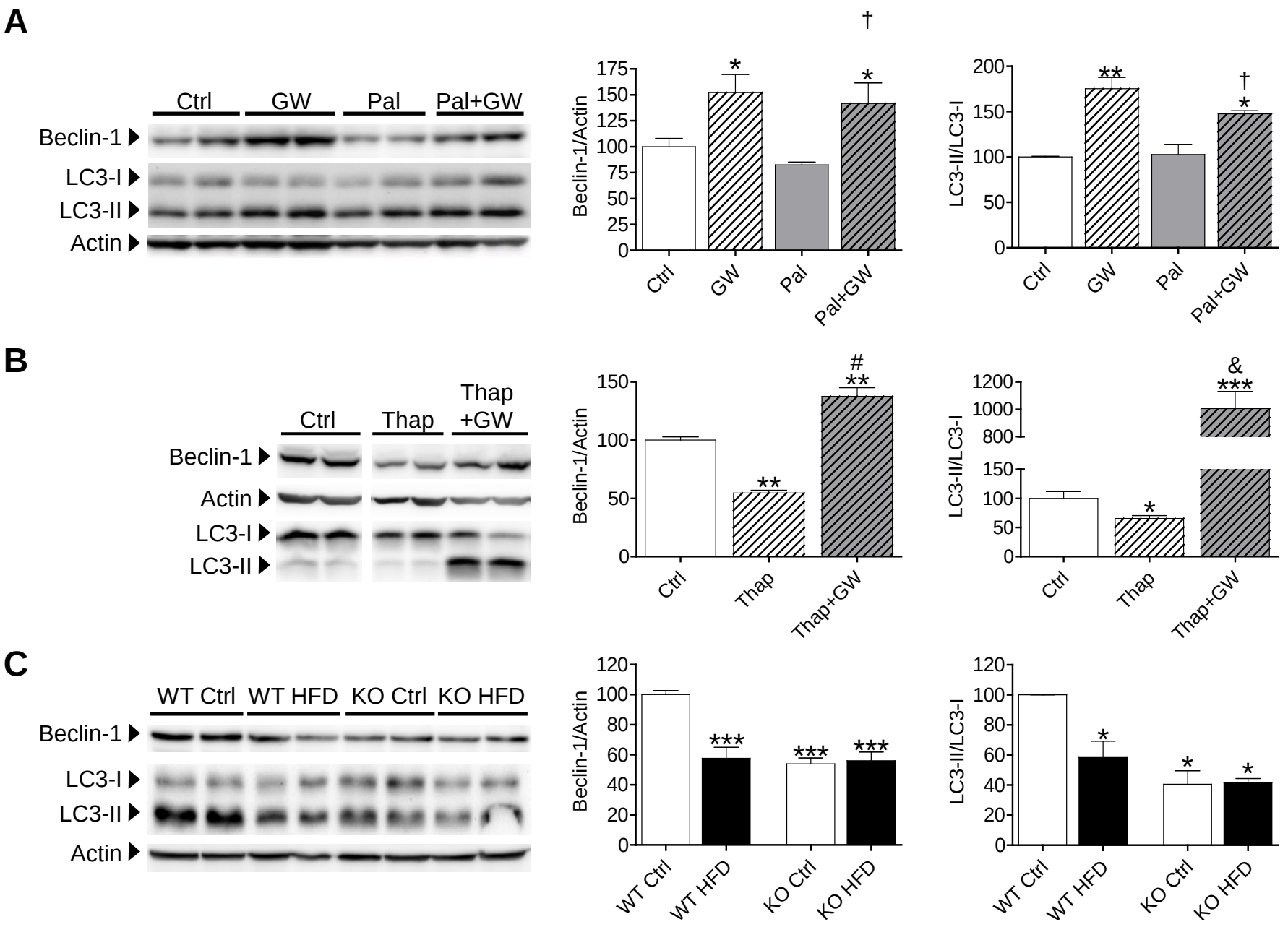
A
Ctrl
GW
Pal
Pal+GW
Beclin-1
LC3-I
LC3-II
Actin
Beclin-1/Actin
LC3-II/LC3-I
B
Ctrl
Thap
Thap +GW
Beclin-1
Actin
LC3-I
LC3-II
Thap+GW
C
WT Ctrl
WT HFD
KO Ctrl
KO HFD

Figure 7

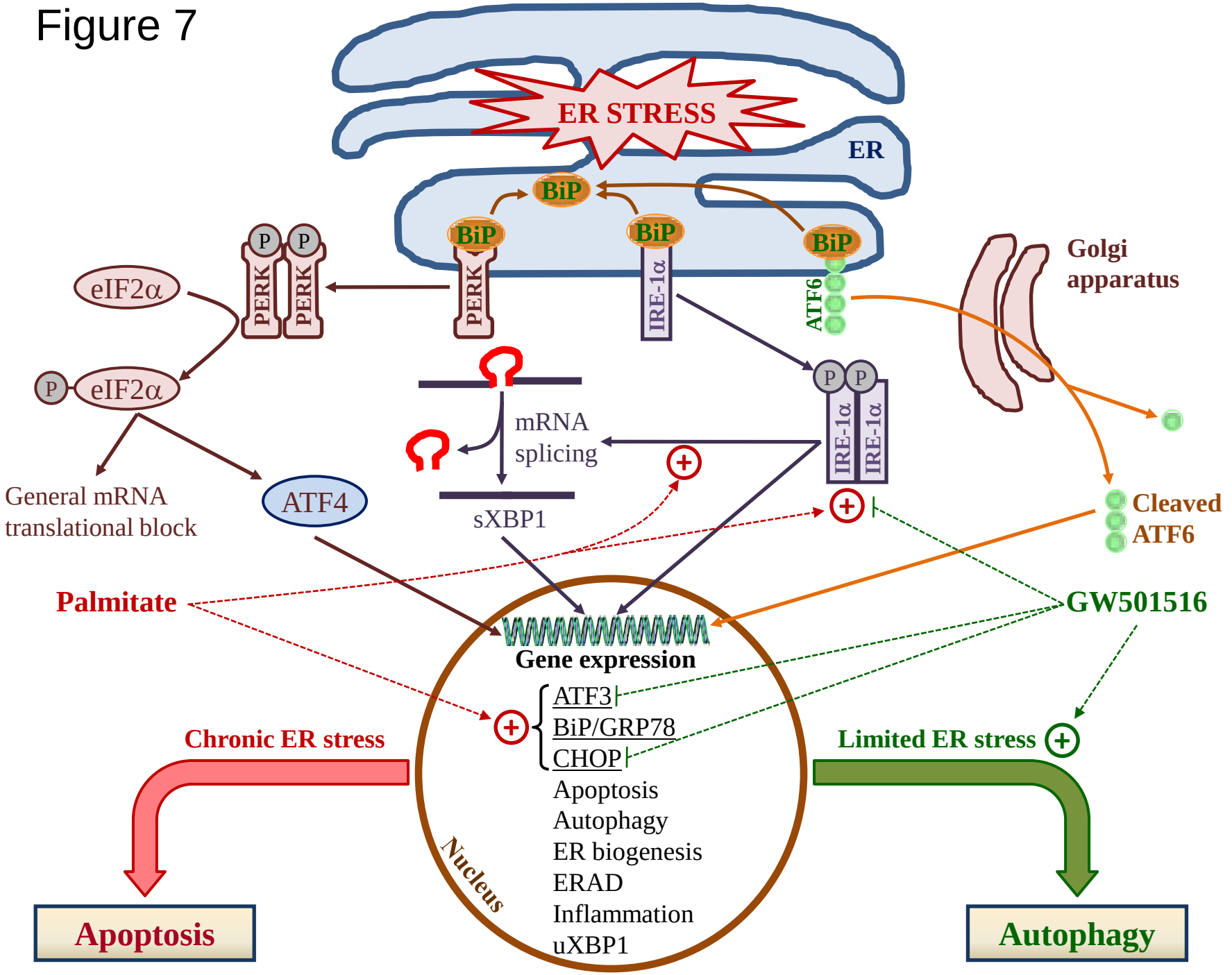
ER STRESS
ER
BiP
BiP
BiP
BiP
PERK
PERK
PERK
IRE-1α
IRE-1α
IRE-1α
ATF6
Golgi apparatus
eIF2α
eIF2α
P
mRNA splicing
sXBP1
General mRNA translational block
ATF4
Cleaved ATF6
Palmitate
GW501516
Gene expression
ATF3
BiP/GRP78
CHOP
Apoptosis
Autophagy
ER biogenesis
ERAD
Inflammation
uXBP1
Nucleus
Chronic ER stress
Limited ER stress
Apoptosis
Autophagy

ONLINE SUPPLEMENTING INFORMATION

Supplemental Figure Legends

Supplemental Fig. 1. AICAR, but not palmitate, induces the PERK/eIF2α branch of the UPR. Western-blot analysis showing protein levels of phosphorylated eIF2α^{Ser51}/eIF2α in total protein extracts isolated from human cardiac AC16 cells incubated for 18 h with palmitate (Pal, 0.25 mmol/L) in the presence or absence of (A) GW501516 (GW, 10 μmol/L) or (B) AICAR (AIC, 2 mmol/L) and Compound C (CC, 30 μmol/L). To show equal loading of protein, the actin signal is included from the same blot. The graphs represent the quantification of the normalized protein levels expressed as a percentage of control samples ±SD. All autoradiograph data are representative of two separate experiments. **P* < 0.05, ***P* < 0.01 and ****P* < 0.001 vs. Ctrl.

Supplemental Fig. 2. AICAR and palmitate display opposite effects on AMPK activity. (A) Western-blot analysis showing protein levels of phosphorylated AMPK^{Thr172}/AMPK and phosphorylated ACC2/ACC2 in total protein extracts isolated from human cardiac AC16 cells incubated for 18 h with palmitate (Pal, 0.25 mmol/L) in the presence or absence of AICAR (AIC, 2 mmol/L) and Compound C (CC, 30 μmol/L). (B) Western-blot analysis showing protein levels of phosphorylated ACC2/ACC2 in total protein extracts isolated from human cardiac AC16 cells incubated for 4h with tunicamycin (Tun, 5 μg/mL) in the presence or absence of AICAR (AIC, 2 mmol/L). To show equal loading of protein, the actin signal is included from the same blot. The graphs represent the quantification of the normalized protein levels expressed as a percentage of control samples ±SD. All autoradiograph data are representative of two separate experiments. **P* < 0.05, ***P* < 0.01 and ****P* < 0.001 vs. Ctrl; †*P* < 0.05 vs. Pal.

Supplemental Fig. 3. The preventive effect of PPARβ/δ activation on palmitate-induced ER stress is AMPK-independent. Human cardiac AC16 cells were incubated for 18 h with palmitate (Pal, 0.25 mmol/L) in the presence or absence of GW501516 (GW, 10 μmol/L), AICAR (AIC, 2 mmol/L) or Compound C (CC, 30 μmol/L). (A) *ATF3*, *BiP/GRP78* and *CHOP* mRNA levels assessed by real-time

RT-PCR analysis. The graphs represent the quantification of the *18S*-normalized mRNA levels, expressed as a percentage of control samples ±SD. (B) Western-blot analysis showing protein levels of phosphorylated AMPK^{Thr172}/AMPK and phosphorylated ACC2/ACC2 in total protein extracts. To show equal loading of protein, the actin signal is included from the same blot. The graphs represent the quantification of the normalized protein levels expressed as a percentage of control samples ±SD. All autoradiograph data are representative of two separate experiments. **P* < 0.05, ***P* < 0.01 and ****P* < 0.001 vs. Ctrl; †*P* < 0.05 and ‡*P* < 0.01 vs. Pal.; #*P* < 0.01 vs. Pal+GW.

Supplemental Fig. 4. PPARβ/δ activation does not attenuate tunicamycin-induced ER stress in human cardiac AC16 cells. Human cardiac AC16 cells were incubated for 4 h with tunicamycin (Tun, 5 μg/mL) in the presence or absence of GW501516 (GW, 10 μmol/L). (A) *sXBP1*, *BiP/GRP78* and *CHOP* mRNA levels assessed by real-time RT-PCR analysis. The graphs represent the quantification of the *18S*-normalized mRNA levels, expressed as a percentage of control samples ±SD. (B) Western-blot analysis showing protein levels of phosphorylated IRE-1α^{Ser724}/IRE-1α in total protein extracts. The graphs represent the quantification of the normalized protein levels expressed as a percentage of control samples ±SD. All autoradiograph data are representative of two separate experiments. **P* < 0.05 and ***P* < 0.01 vs. Ctrl.

Supplemental Fig. 5. HFD feeding and PPARβ/δ suppression downregulate AMPK activity in the heart of mice. (A) *sXBP1* mRNA levels in samples obtained from the heart of wild-type (WT) or knockout PPARβ/δ (KO) mice fed a standard chow diet (Ctrl) or a saturated fatty acid-rich diet (HFD) for two months. (B) Western-blot analysis showing protein levels of phosphorylated AMPK^{Thr172}/AMPK and phosphorylated ACC2/ACC2 in total protein extracts obtained from the same samples depicted in panel A. To show equal loading of protein, the actin signal is included from the same blot. The graphs represent the quantification of the normalized protein levels expressed as a percentage of control samples ±SD. All autoradiograph data are representative of two separate experiments. **P* < 0.05, ***P* < 0.01 and ****P* < 0.001 vs. WT Ctrl.

Supplemental Fig. 6. Palmitate does not induce apoptosis in human cardiac AC16 cells. Human cardiac AC16 cells were incubated for 18 h with palmitate (Pal, 0.25 mmol/L) in the presence or absence of GW501516 (GW, 10 μmol/L). (A) *Bax*, *Bim* and *Puma* mRNA levels assessed by real-time RT-PCR analysis. The graphs represent the quantification of the *18S*-normalized mRNA levels, expressed as a percentage of control samples ±SD. Western-blot analysis showing the proteolysis of α-spectrin (B) or the protein levels of Bax and Bcl-2 (C) in total protein extracts. To show equal loading of protein, the actin signal is included from the same blot. The graph represent the quantification of the normalized protein levels expressed as a percentage of control samples ±SD. All autoradiograph data are representative of two separate experiments. ‡$P < 0.01$ vs. Pal.

Supplemental Fig. 7. Autophagy is not induced after AMPK activation in human cardiac AC16 cells. (A) *Beclin-1* and *LC3* mRNA levels in human cardiac AC16 cells incubated for 18 h with palmitate (Pal, 0.25 mmol/L) and GW501516 (GW, 10 μmol/L). (B) and (C) western-blot analysis showing beclin-1 levels in human cardiac AC16 cells incubated for 4 h with tunicamycin (Tun, 5 μg/mL) and GW501516 (GW, 10 μmol/L) (B), or palmitate (Pal, 0.25 mmol/L) and AICAR (AIC, 2 mmol/L) (C). To show equal loading of protein, the actin signal is included from the same blot. The graph represents the quantification of the normalized protein levels expressed as a percentage of control samples ±SD. *$P < 0.05$ vs. Ctrl; †$P < 0.05$ vs. Tun.

Supplemental Fig. 8. Thapsigargin induces ER stress in human cardiac cells. Western-blot analysis showing the protein levels of BiP/GRP78 and CHOP in total protein extracts obtained from human cardiac AC16 cells incubated for 18 h with tahpsigargin (Thap, 1 μmol/L) and GW501516 (GW, 10 μmol/L). To show equal loading of protein, the actin signal is included from the same blot. The graphs represent the quantification of the normalized protein levels expressed as a percentage of control samples ±SD. **$P < 0.01$ and ***$P < 0.001$ vs. Ctrl; †$P < 0.05$ vs. Thap.

Supplemental Fig. 9. eIF2α phosphorylation at Ser51 residue is enhanced in the heart of mice fed a HFD or after PPARβ/δ suppression. Western-blot analysis showing protein levels of phosphorylated $eIF2\alpha^{Ser51}$/eIF2α in total protein extracts obtained from the heart of wild-type (WT) or knockout PPARβ/δ (KO) mice fed a standard chow diet (Ctrl) or a saturated fatty acid-rich diet (HFD) for two months. To show equal loading of protein, the actin signal is included from the same blot. The graph represents the quantification of the normalized protein levels expressed as a percentage of control samples ±SD.. **P* < 0.05 and ***P* < 0.01 vs. WT Ctrl.

Supplemental Fig. 10. The NF-κB inhibitor parthenolide attenuates palmitate-induced *ATF3* and *CHOP* expression. *ATF3* and *CHOP* mRNA levels assessed by real-time RT-PCR analysis in AC16 cells incubated for 18 h with palmitate (Pal, 0.25 mmol/L) in the presence or absence of parthenolide (Parth, 10 μmol/L). The graphs represent the quantification of the *18S*-normalized mRNA levels, expressed as a percentage of control samples ±SD. ***P* < 0.01 and ****P* < 0.001 vs. Ctrl; †*P* < 0.01 and ‡*P* < 0.001 vs. Pal.

Supplemental Table

Table S1. Primers used for the real-time RT-PCR reactions.

Gene	Forward primers	Reverse primers
Mice		
APRT	5'-CAGCGGCAAGATCGACTACA-3'	5'-AGCTAGGGAAGGGCCAAACA-3'
BiP/GRP78	5'-CAGATCTTCTCCACGGCTTC-3'	5'-GCAGGAGGAATTCCAGTCAG-3'
CHOP	5'-CGAAGAGGAAGAATCAAAAACCTT-3'	5'-GCCCTGGCTCCTCTGTCA-3'
Human		
18S	5'-GCCGCTAGAGGTGAAATTCTTG-3'	5'-CATTCTTGGCAAATGCTTTCG-3'
ATF3	5'-AAGAACGAGAAGCAGCATTTGAT -3'	5'- TTCTGAGCCCGGACAATACAC-3'
Bax	5'- TGGAGCTGAAGAGGATGATTG-3'	5'- GCTGCCACTCGGAAAAAGAC-3'
Beclin-1	5'- TGGTGTCTCTCGCAGATTCATC-3'	5'- GCCTCCCCAATCAGAGTGAAG-3'
Bim	5'-GCGTATTGGAGACGAGTTTAACG-3'	5'-GGTCTTCGGCTGCTTGGTAA-3'
BiP/GRP78	5'-ACTATTGCTGGCCTAAATGTTATGAG-3'	5'-TTATCCAGGCCATAAGCAATAGC-3'
CHOP	5'-GGAAATGAAGAGGAAGAATCAAAAAT-3'	5'-GTTCTGGCTCCTCCTCAGTCA-3'
LC3	5'-GAGAAGCAGCTTCCTGTTCTGG-3'	5'-GTGTCCGTTCACCAACAGGAAG-3'
Puma	5'-GGGTCCCCTGCCAGATTT-3'	5'-CAGGAGTCCCATGATGAGATTG-3'

Supplementary Figure S1

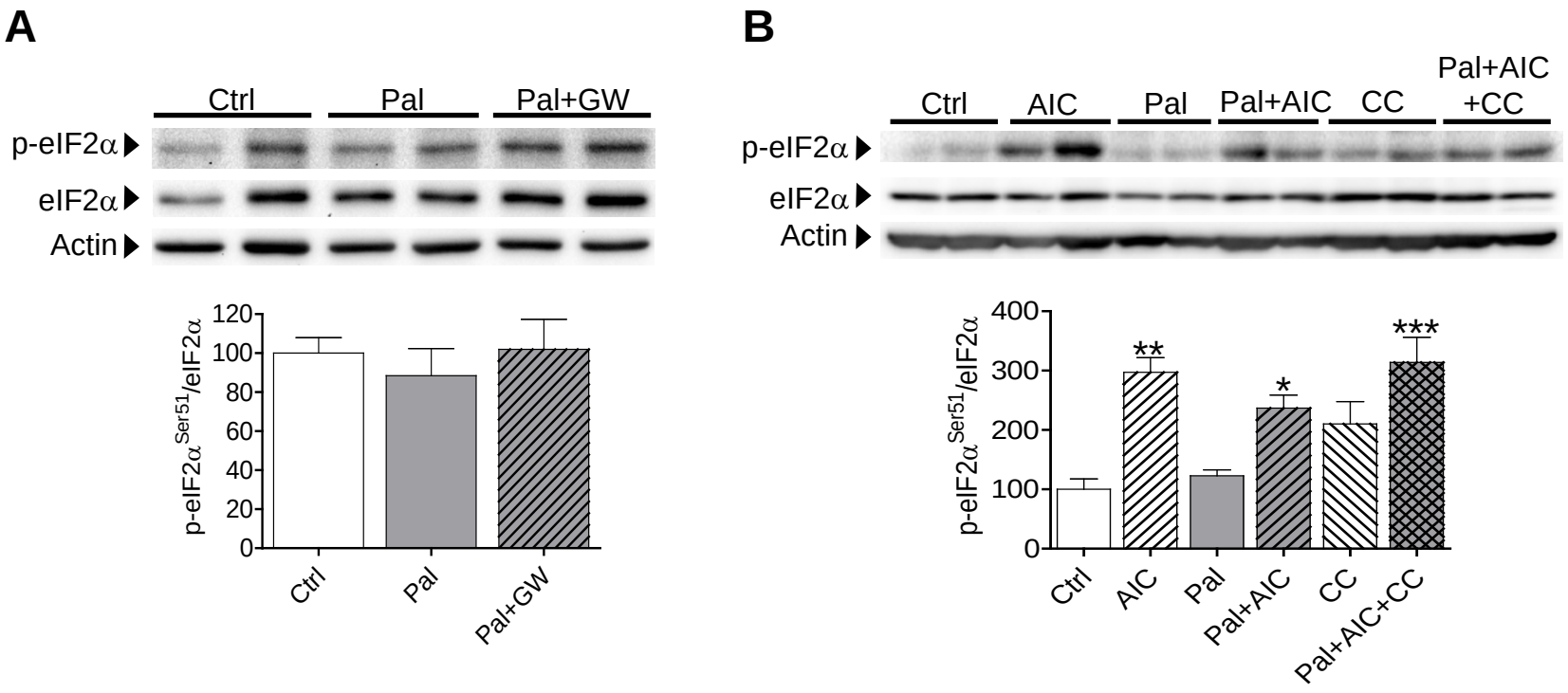

Supplementary Figure S2

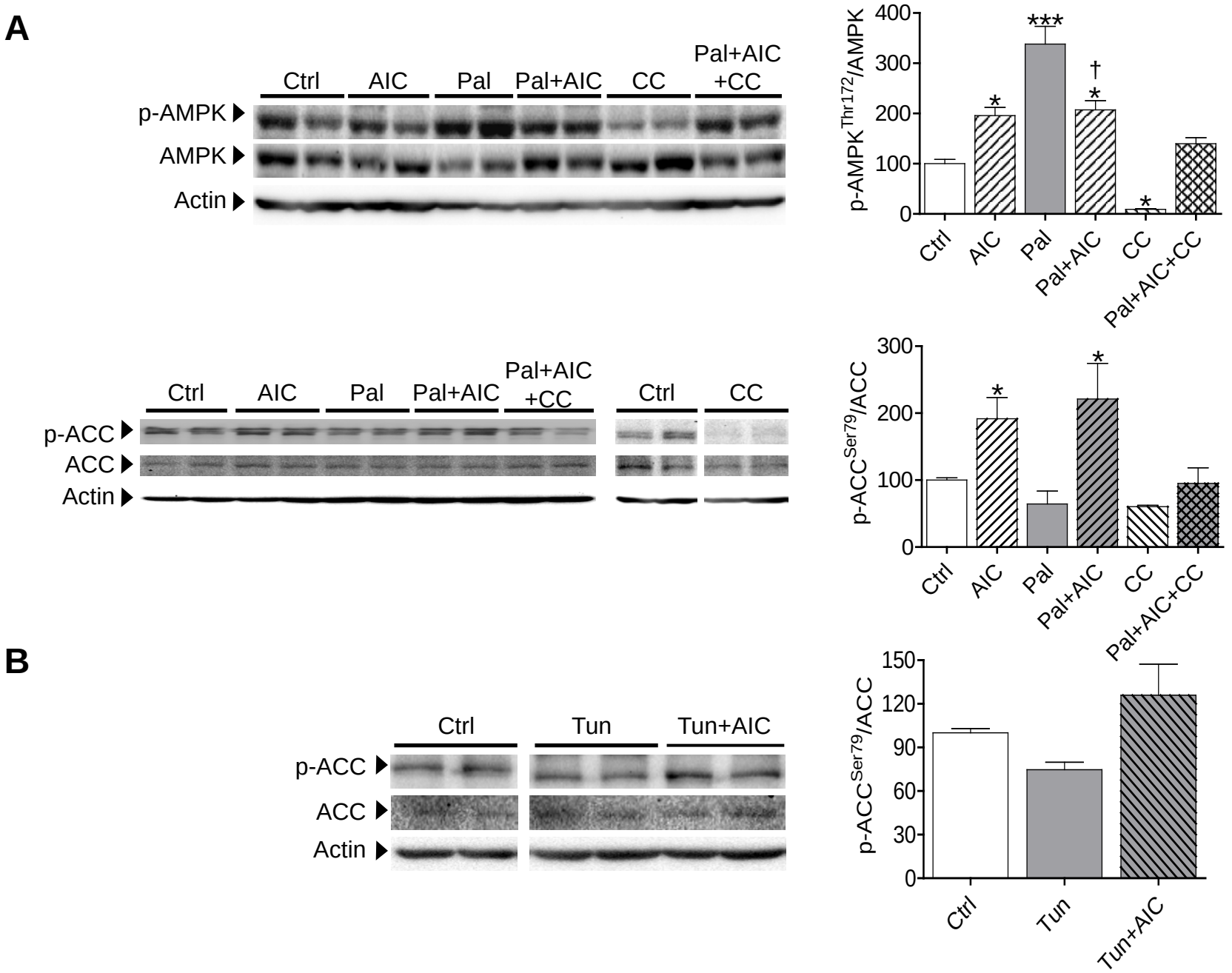

Supplementary Figure S3

A

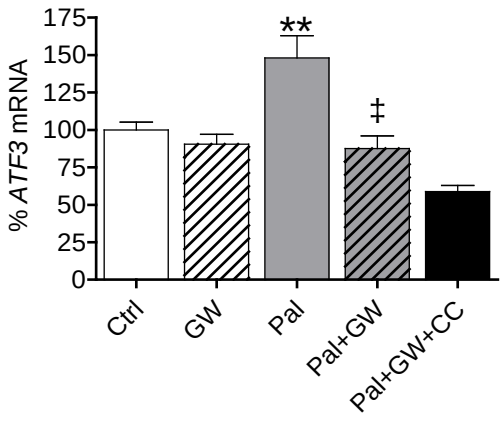

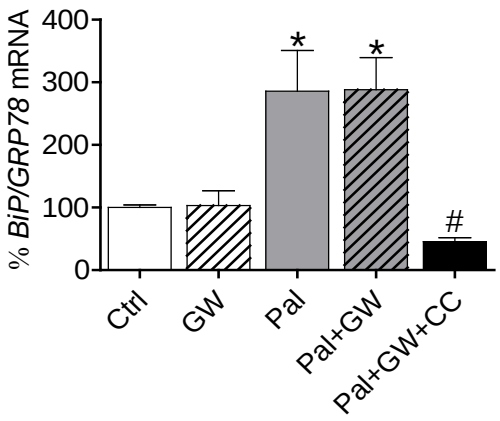

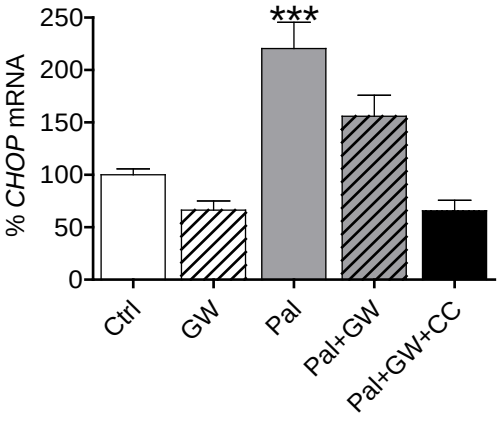

B

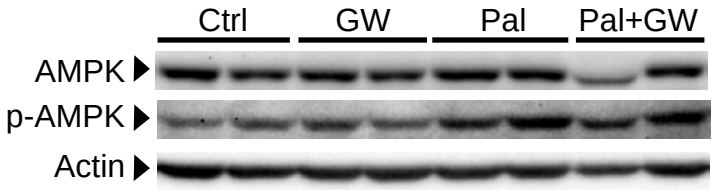

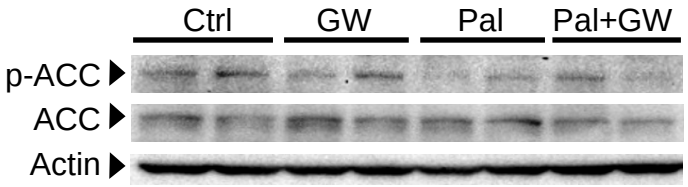

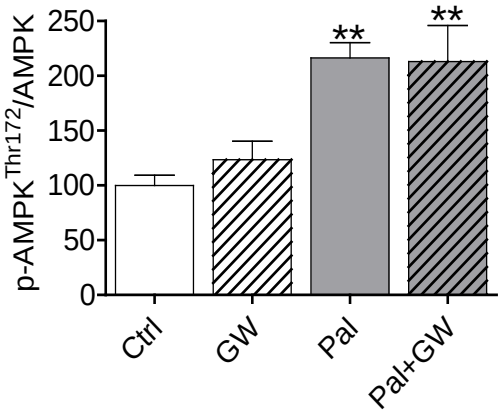

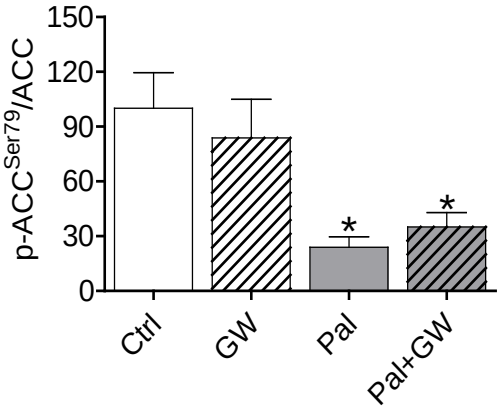

Supplementary Figure S4

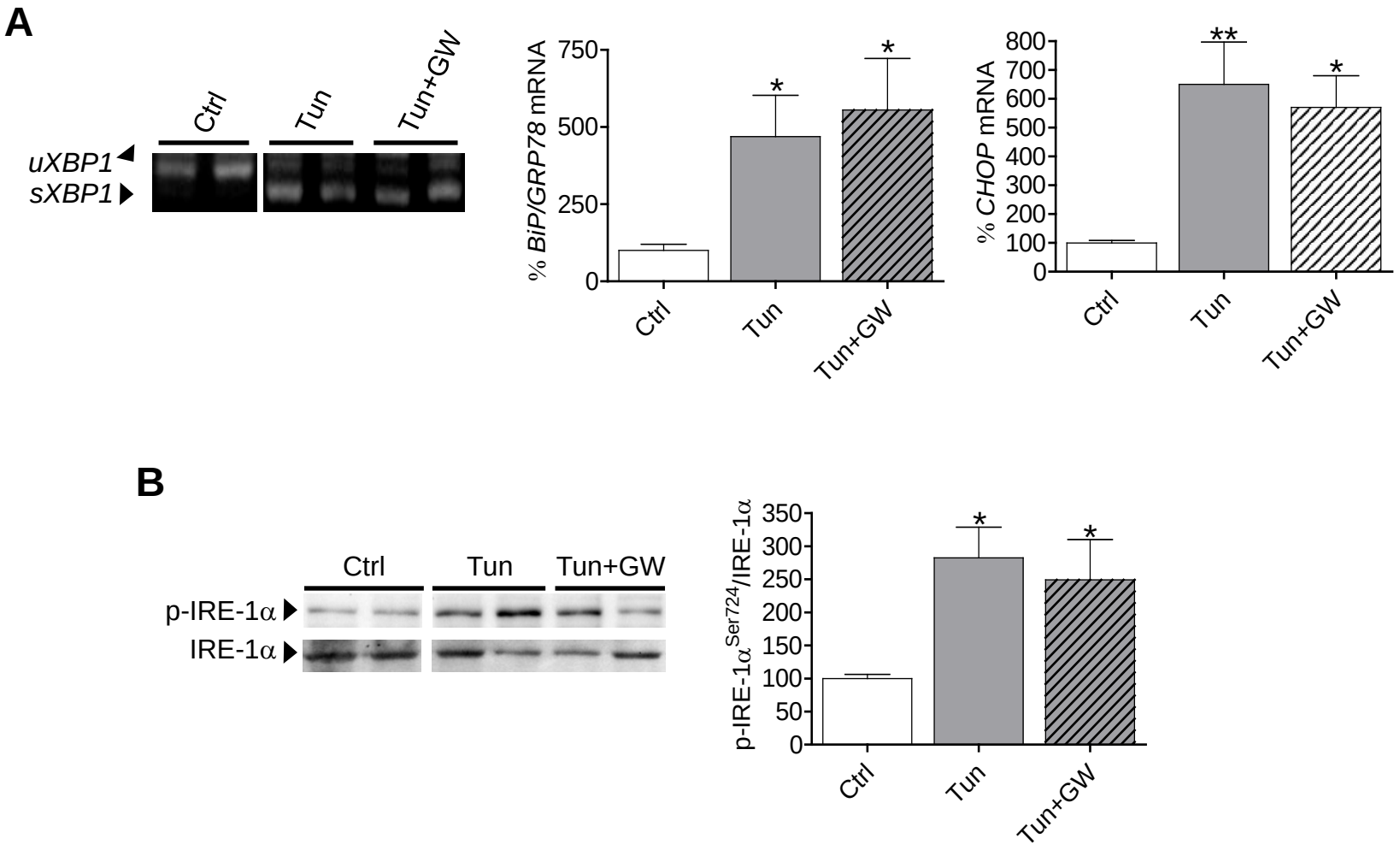

Supplementary Figure S5

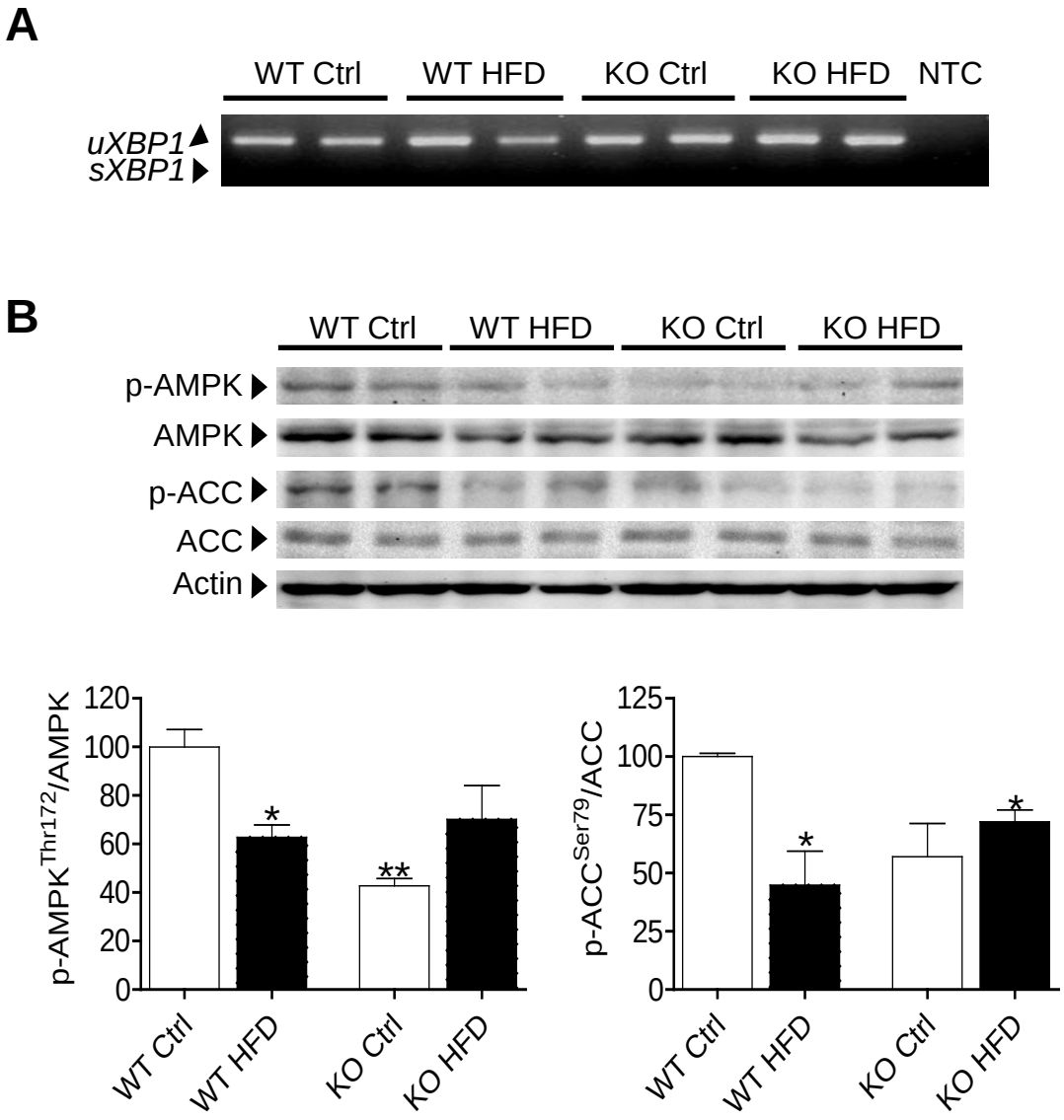

Supplementary Figure S6

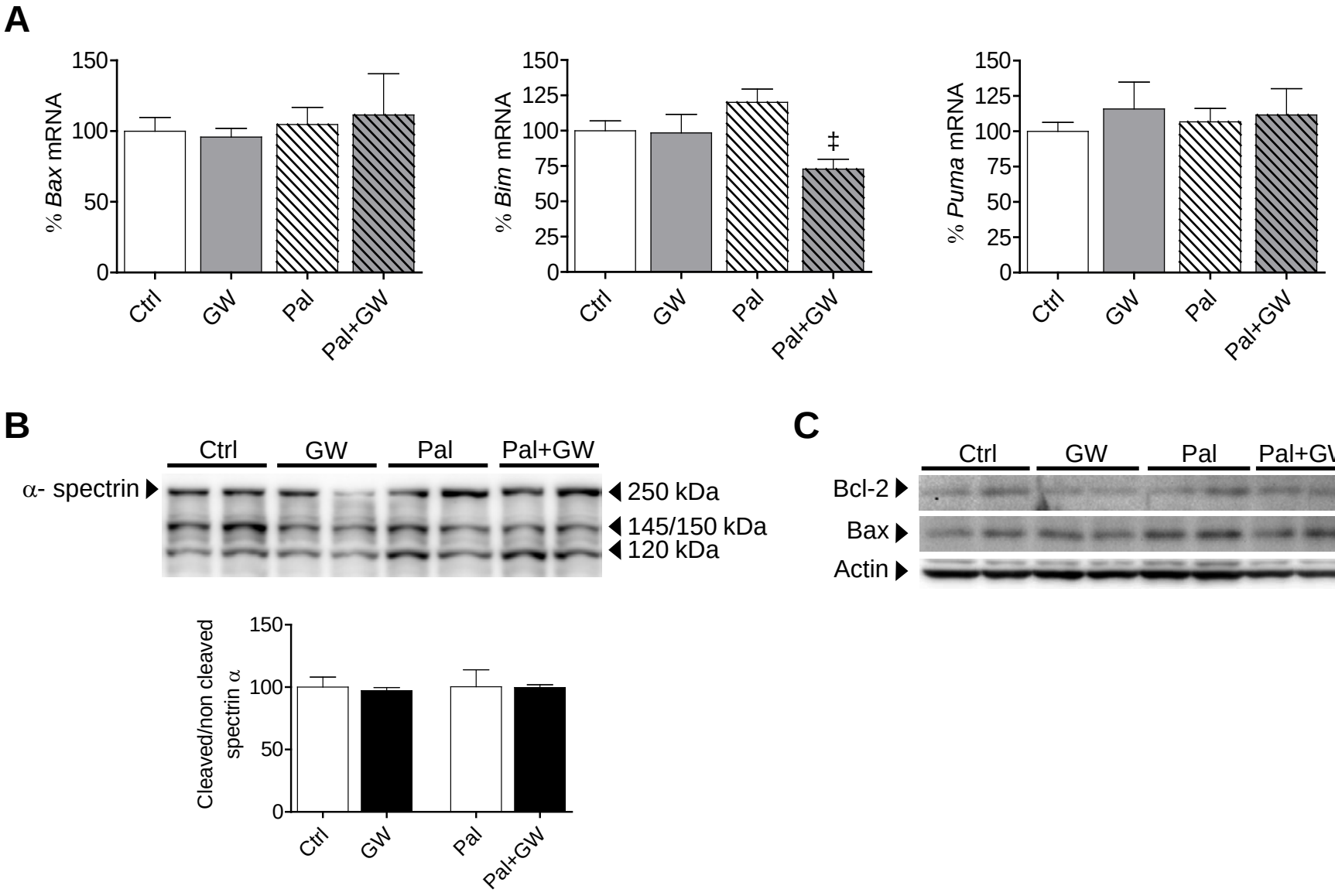

Supplementary Figure S7

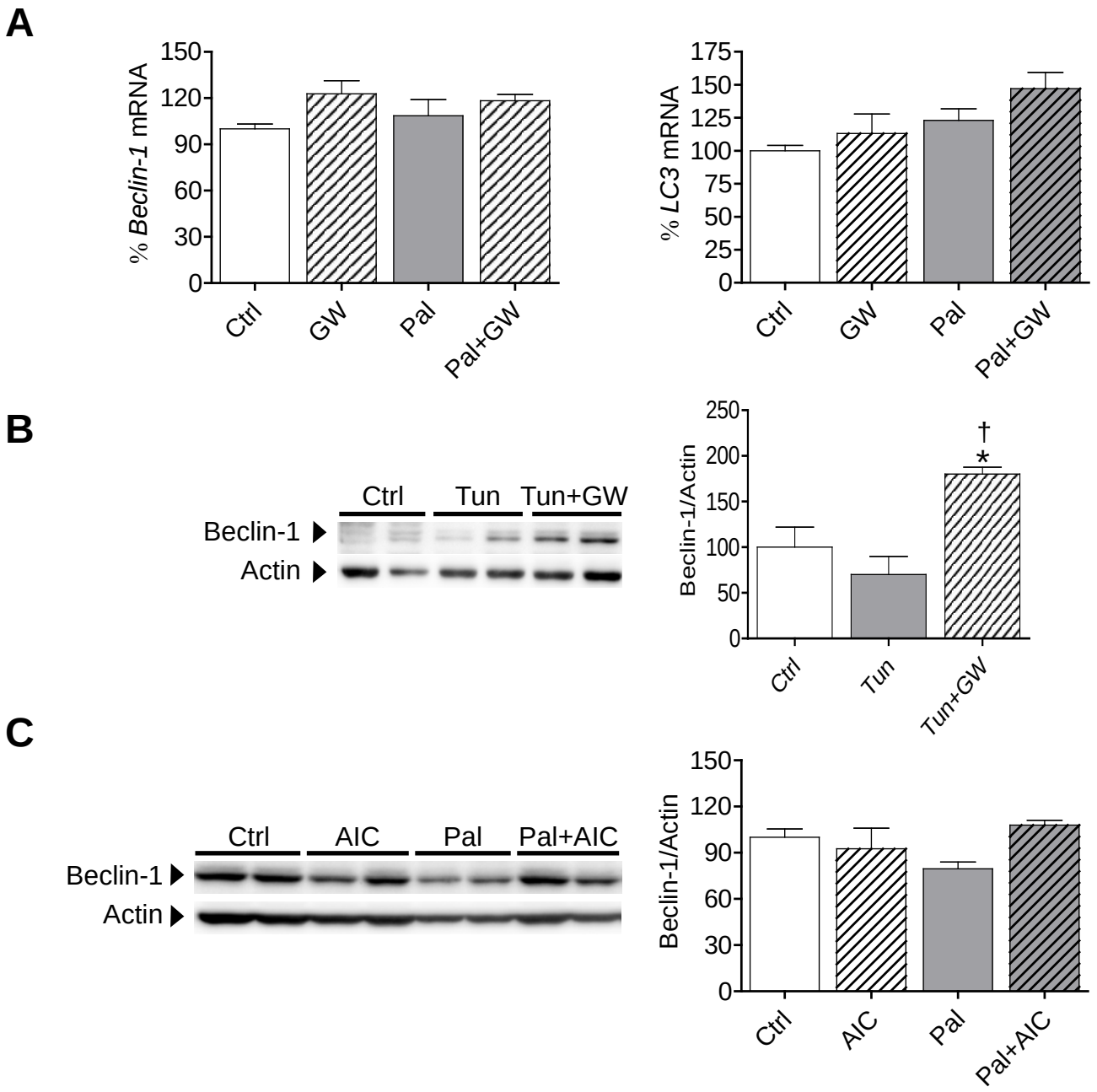

Supplementary Figure S8

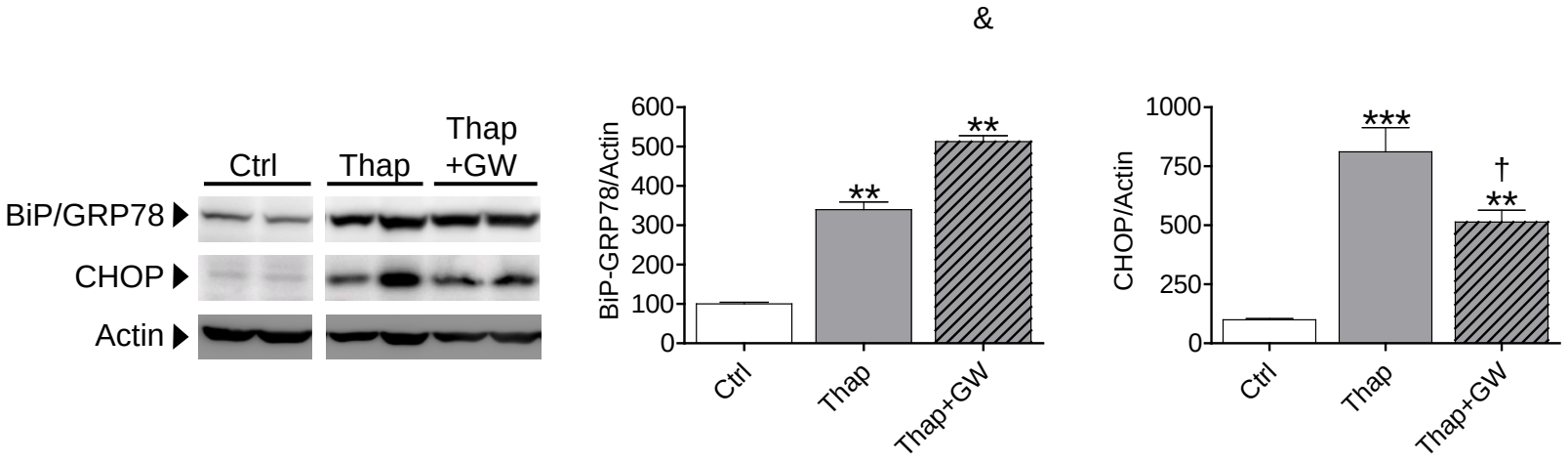

Supplementary Figure S9

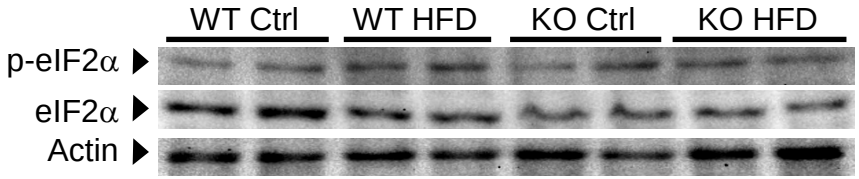

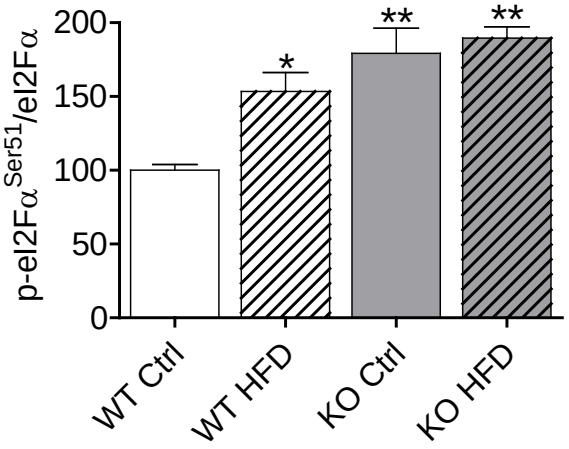

Supplementary Figure S10